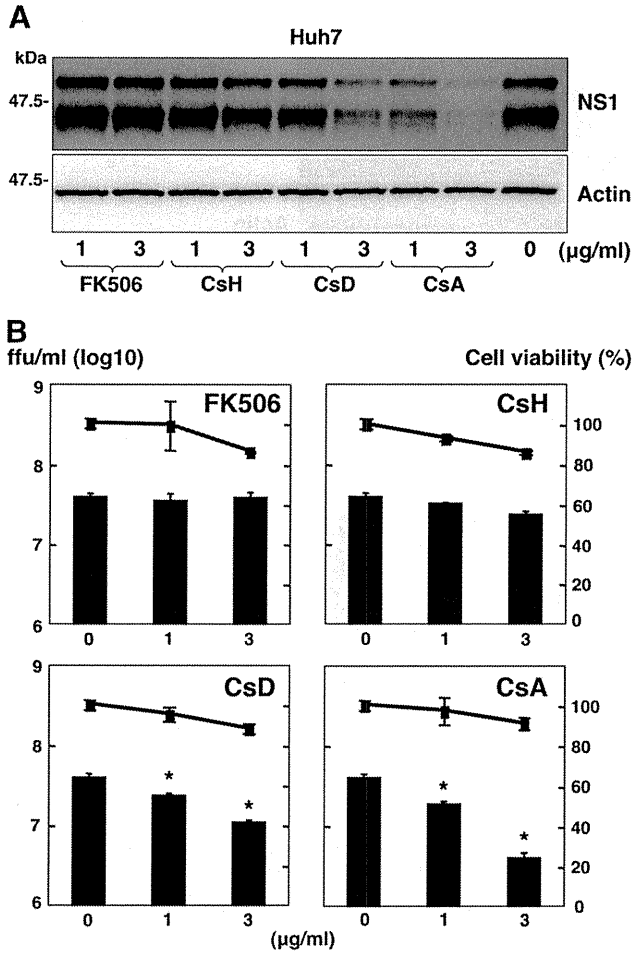

Fig. 2. CsA inhibits JEV propagation through the inhibition of Cyps. Huh7 cells were infected with JEV at an MOI of 0.1 for 1 h and then treated with 10% FBS DMEM containing the indicated concentrations of CsA, CsD, CsH, or FK506 for 48 h. The propagation of JEV was evaluated by immunoblotting (A) and focus-forming assay (B). The results are representative of three independent assays, with the error bars indicating the standard deviations. Asterisks indicate significant differences (*$P<0.01$).

to CypC compared to the level in the cells transfected with the control siRNA (Fig. 3B). JEV was inoculated into cells transfected with the siRNA at 48 h post-transfection and the cells and culture supernatants were harvested at 48 h post-infection. Expression of JEV NS1 was most effectively decreased by the knockdown of CypB, followed by CypC, and knockdown of CypA resulted in a marginal reduction of NS1 expression compared to the control siRNA (Fig. 3C). Furthermore, the production of JEV was also effectively suppressed in cells with knockdown of CypB, followed by those with knockdown of CypC and CypA (Fig. 3D). These results suggest that CypB plays an important role in the propagation of JEV. To further confirm the effect CypB on the propagation of JEV, we established stable knockdown cell lines expressing a short hairpin RNA (shRNA) targeted to CypB. Consistent with the data from transient knockdown experiments, both expression of NS1 and virus production were significantly reduced in the CypB-knockdown cell lines (Bose et al., 2003; Castro et al., 2003) in accordance with the reduction of CypB (Fig. 4A and B). There was no significant difference in cell growth among the cell lines (Fig. 4C).

PPIase activity of CypB is crucial for the propagation of JEV

The PPIase activity of Cyps is suggested to catalyze the proper folding of certain proteins (Andreotti, 2003; Wang and Heitman, 2005). It has been demonstrated that PPIase activity of Cyps is required for HCV replication (Chatterji et al., 2009; Kaul et al., 2009; Watashi et al., 2005). To examine the effect of the PPIase activity of CypB on the propagation of JEV, we constructed an expression plasmid encoding a PPIase-defective CypB in which the Arg^{62} was replaced with Ala, because the Arg^{62} in CypB has been shown to be critical for PPIase catalytic activity (Carpentier et al., 1999). Each of the expression plasmids encoding the FLAG-tagged wild- or Ala^{62}-CypB carrying the silent mutations resistant to the siRNA was introduced into the stable CypB-knockdown cell line (Bose et al., 2003) and cultured for a week in the presence of neomycin. Although expression of both endogenous and exogenous CypB was detected at a similar level (Fig. 4D), JEV production was partially rescued by introducing the wild-CypB but not the Ala^{62}-CypB (Fig. 4E). These results indicate that the PPIase activity of CypB is crucial for the propagation of JEV.

CypB participates in the replication but not in the entry of JEV

To further examine the effect of CsA on the JEV life cycle, we generated a subgenomic replicon of JEV to assess the effect of CsA on the JEV RNA replication (Fig. 5A). The replicon cells treated with CsA for 6 days exhibited a significant reduction of NS1 expression compared to the non-treated cells (Fig. 5B). The replicon RNA transcribed from the pJErepIRESpuro was transfected into the stable CypB-knockdown (#4) or control cell lines and incubated for 3 weeks in the presence of puromycin. A few colony formation was detected in the CypB-knockdown cell line, in contrast to the abundant colony formation in the control cell line (Fig. 5C). These results suggest that CypB is required for the efficient replication of JEV.

Next, to examine the impact of CypB on the entry of JEV, we generated pseudotype VSVs bearing envelope proteins of JEV (JEVpv) or VSV (VSVpv). Because these viruses possess the luciferase gene, the infectivity can be assessed by the luciferase activity (Tani et al., 2010). Huh7 cells pretreated with various concentrations of CsA were infected with JEVpv or VSVpv, and the infectivity was assessed by the expression of luciferase. There was no significant effect of CsA on the infection of either pseudotype virus (Fig. 5D). Similarly, no effect was observed on the infection of the pseudotype viruses in the CypB-knockdown cell lines (Fig. 5E). Collectively, these results clearly indicate that CypB participates in the replication but not in the entry of JEV.

CypB interacts with the JEV NS4A protein

Many viruses have been shown to utilize Cyps through the interaction with their viral proteins. For example, HCV recruits CypA and CypB to enhance viral RNA replication through the interaction with NS5A and NS5B, respectively (Chatterji et al., 2009; Kaul et al., 2009; Watashi et al., 2005; Yang et al., 2008). To determine whether the JEV proteins interact with CypB, we prepared expression plasmids encoding each of the JEV nonstructural proteins involved in the viral RNA replication. FLAG-tagged CypB was co-expressed with each of the HA-tagged JEV nonstructural proteins in 293T cells and immunoprecipitated with anti-HA antibody. The precipitates were subjected to immunoblotting by using either anti-FLAG or anti-HA antibodies. CypB was co-precipitated with the JEV NS4A protein but not with other proteins (Fig. 6A). Furthermore, interaction of CypB with NS4A was reduced in the immunoprecipitation analysis in the presence of CsA (Fig. 6B). To gain more insight into the interaction between CypB and NS4A, the intracellular localization of these proteins was examined by confocal microscopy. Huh7 cells were transfected with an expression plasmid encoding HA-tagged NS4A or an empty vector and fixed at 48 h post-transfection. Endogenous CypB was detected in the perinuclear region together with NS4A protein. In addition, NS4A colocalized with ER marker protein, calnexin (Fig. 6C). These results suggest that NS4A protein interacts with CypB at the replication complex localized in the ER.

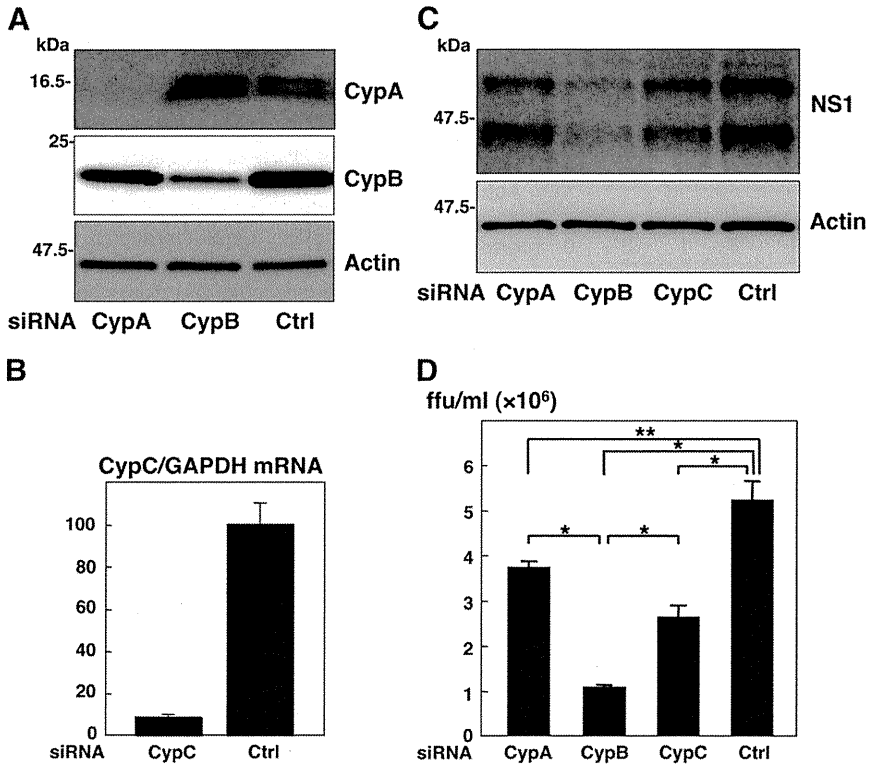

Fig. 3. CypB plays an important role in the propagation of JEV. (A) Knockdown of endogenous CypA and CypB by siRNA. Huh7 cells were transfected with 35 nM of siRNA targeted to CypA, CypB, or a non-specific control. Cell lysates after 96 h post-transfection were analyzed for expression of CypA, CypB, or actin by immunoblotting. (B) Huh7 cells transfected with 35 nM of siRNA targeted to CypC or a non-specific control were harvested at 24 h post-transfection. CypC mRNA levels were determined by quantitative real-time PCR. The level of CypC mRNA was normalized to the amount of GAPDH mRNA and expressed as a percentage of the control value. (C, D) Huh7 cells were transfected with siRNA targeted to CypA, CypB, or CypC and infected with JEV at an MOI of 0.1 at 48 h post-transfection. The propagation of JEV was determined by immunoblotting (C) and focus-forming assay (D). The results are representative of three independent assays, with the error bars indicating the standard deviations. Asterisks indicate significant differences (*$P<0.01$; **$P<0.05$).

Discussion

In this study, we have shown that CsA inhibits the replication of JEV through the inhibition of the PPIase activity of Cyps. A previous study showed that CsA does not induce interferon in Huh7 cells (Nakagawa et al., 2005), suggesting that the antiviral activity of CsA on the propagation of JEV relies on the inhibition of Cyps. Cyps are highly conserved PPIases that catalyze the *cis-trans* isomerization of peptide bonds to facilitate certain protein foldings (Andreotti, 2003; Wang and Heitman, 2005) and are involved in the correct folding of host and viral proteins. Among the Cyp isoforms, CypA and CypB are the most abundantly expressed in cells and play key roles in the propagation of various viruses. CypA is incorporated into HIV, influenza A virus, VSV, and VV to regulate their replication (Bose et al., 2003; Castro et al., 2003; Damaso and Moussatche, 1998; Franke et al., 1994; Liu et al., 2009; Thali et al., 1994). CypB is incorporated into MV particles to facilitate an efficient infection (Watanabe et al., 2010). Both CypA and CypB have been shown to serve as host factors involved in the replication of HCV through the interaction with NS5A and NS5B (Chatterji et al., 2009; Kaul et al., 2009; Watashi et al., 2005; Yang et al., 2008).

Recently, Qing et al. reported that CypA plays an important role in the replication of flaviviruses such as WNV, YFV, and DENV. The PPIase activity of CypA was shown to be crucial for the efficient replication of the viruses, indicating that CypA acts as a molecular chaperone for the viral and host proteins required for an effective RNA replication (Qing et al., 2009). Indeed, knockdown of CypA suppressed the JEV propagation in this study, but that of CypB exhibited more potent impairment of the JEV propagation, suggesting that CypB plays a crucial role in the propagation of JEV. However, we could not exclude the possibility of the involvement of other Cyps in the replication of JEV. Multiple Cyps have been shown to involved in the life cycle of HCV (Gaither et al., 2010; Nakagawa et al., 2005) and the knockdown experiment of Cyps in this study suggests that not only CypB, but also CypC and CypA are involved in the propagation of JEV. At least 16 Cyps have been shown to participate in various cellular functions in humans (Wang and Heitman, 2005), and therefore, further studies to clarify the precise function of these Cyps in the life cycle of the flaviviruses are needed.

In addition to Cyps, flavivirus recruits several host chaperones for an efficient propagation. HSP70 and HSP90 have been identified as comprising the DENV receptor complex in human cell lines. These chaperones presumably facilitate the viral envelope dimer–trimer transition after the binding of the envelope protein to the cellular receptor (Reyes-Del Valle et al., 2005). Moreover, inhibition of the interaction between the ER chaperone calnexin and JEV glycoproteins has been suggested to affect the folding of viral proteins, leading to a reduction in the mortality rate in a mouse model of lethal infection (Wu et al., 2002). It has been reported that ER chaperones including BiP, calnexin, and calreticulin interact with the DENV envelope protein, and that knockdown of these chaperones decreased viral production (Limjindaporn et al., 2009). In addition, BiP was shown to be upregulated in cells infected with DENV to facilitate viral production (Wati et al., 2009), and BiP and calreticulin have been associated with CypB (Zhang and Herscovitz, 2003). Therefore, these ER resident chaperones are considered to play important roles in the flavivirus replication through the proper folding of the viral and host proteins making up the viral RNA replication complex.

Lack of recovery of JEV propagation in the CypB-knockdown cell lines by the expression of the PPIase-deficient CypB mutant suggests that PPIase activity is crucial for the JEV production. Although the PPIase activity of CypA has been shown to be required for flavivirus replication

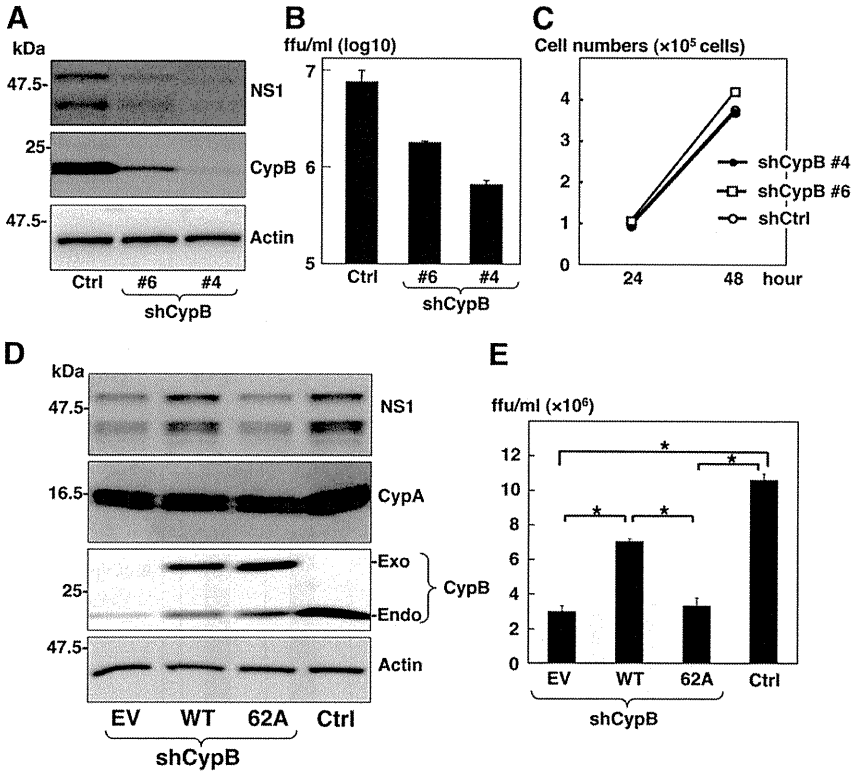

Fig. 4. PPIase activity of CypB is crucial for the propagation of JEV. Huh7 cell lines expressing shRNA targeted to CypB or the control were infected with JEV at an MOI of 0.1 for 1 h and cultured in 10% FBS DMEM for 48 h. The expressions of NS1, CypB, and actin were detected by immunoblotting (A). The propagation of JEV was determined by focus-forming assay (B). Growth kinetics of the stable CypB-knockdown cell lines were determined by the method of trypan blue dye exclusion (C). The stably knocked-down cell lines were transfected with the siRNA-resistant FLAG-tagged wild- or Ala^{62}-CypB, or empty vector and cultured for 1 week in the presence of 1 μg/ml puromycin. The remaining cells were infected with JEV at an MOI of 1. The expressions of NS1, CypA, endogenous and exogenous CypBs, and actin were detected by immunoblotting (D). Virus production in the culture supernatant at 36 h post-infection was determined by a focus-forming assay (E). The results are representative of three independent assays, with the error bars indicating the standard deviations. Asterisks indicate significant differences (*$P<0.01$).

through the interaction with the NS5 polymerase (Qing et al., 2009), CypB was colocalized and specifically co-immunoprecipitated with JEV NS4A. CypA is abundantly expressed in the cytoplasm of mammalian cells (Galigniana et al., 2004) and NS5 is predominantly detected on the cytoplasmic side of the ER (Zhang et al., 1992). Thus, it is conceivable that an interaction between CypA and NS5 occurs on the cytoplasmic side of the ER. On the other hand, CypB is localized in the ER lumen and targeted to the secretory pathway via its ER signal sequence (Price et al., 1994, 1991). NS4A is predicted to be a three-transmembrane protein with its C-terminal end localized in the ER lumen (Miller et al., 2007). Therefore, it is plausible that CypB interacts with NS4A within the ER lumen and confers proper folding to form the RNA replication complex of JEV. Expression of DENV NS4A alone has been shown to induce rearrangement of the cytoplasmic membrane to form the convoluted membrane required for viral replication (Roosendaal et al., 2006). It might be feasible to speculate that JEV NS4A undergoes conformational change through the interaction with CypB and induces formation of the convoluted membrane in the ER essential for genome replication of JEV. It was reported that HCV NS5A from CsA resistant mutant exhibits an enhanced interaction with CypB and NS5B facilitates a stronger binding of the mutant NS5A to endogenous CypB than wild-type in cell culture (Fernandes et al., 2010). Study of the molecular mechanism underlying the CsA resistant of JEV may shed light on the complex interaction among Cyps and viral proteins.

In conclusion, we have demonstrated that CsA suppresses the propagation of JEV by inhibiting the interaction between CypB and NS4A, which is required for viral RNA replication. Further studies are needed to elucidate the precise molecular mechanism underlying the involvement of cellular Cyps in the efficient propagation of JEV. Three inhibitors of the PPIase activity of Cyps, DEBIO-025, SCY635, and NIM811, are currently under clinical trial for the treatment of hepatitis C patients (Puyang et al., 2010). The PPIase inhibitor may be an attractive therapeutic target for the treatment of patients infected with not only HCV but also other flaviviruses.

Materials and methods

Plasmids

The human CypB gene was amplified from the total cDNA of Huh7 by PCR using *LA taq* (Takara Bio Inc., Shiga, Japan) and cloned into pcDNA3.1 and pCAGPM (Mori et al., 2007). The plasmids encoding the NS1, NS2A, NS2B, NS3, NS4A, NS4B and NS5 of the JEV AT31 strain were generated by PCR and cloned into pCAGPM. The pSilencer-CypB, carrying an shRNA targeted to CypB under the control of the U6 promoter, was constructed by cloning of the oligonucleotide pair 5′-GATCCGGTGGAGAGCACCAAGACATTCAAGAGATGTCTTGGTGCTCTC-CACCTTTTTTGGAAA-3′-5′-AGCTTTTCCAAAAAAGGTGGAGAGCACCAA-GACATCTCTTGAATGTCTTGGTGCTCTCCACCG-3′ between the *Bam*HI and *Hind*III sites of pSilencer 2.1-U6 hygro (Ambion, Austin, TX). A plasmid coding a mutant CypB resistant to shRNA was prepared by insertion of four silent mutations (the nucleotides at positions 543, 549, 555, and 561 were changed from G to A, G to A, C to G, and A to C, respectively) into CypB cDNA by the method of splicing by overlap extension (Ho et al., 1989). The pSilencer negative-control plasmid (Ambion) has no homology to any human gene. The pJErep plasmid was kindly provided by Dr. Konishi (Kobe University, Kobe, Japan). A puromycin-resistant gene under the internal ribosomal entry site (IRES) of encephalomyocarditis virus was inserted into pJErep and designated as pJErepIRESpuro.

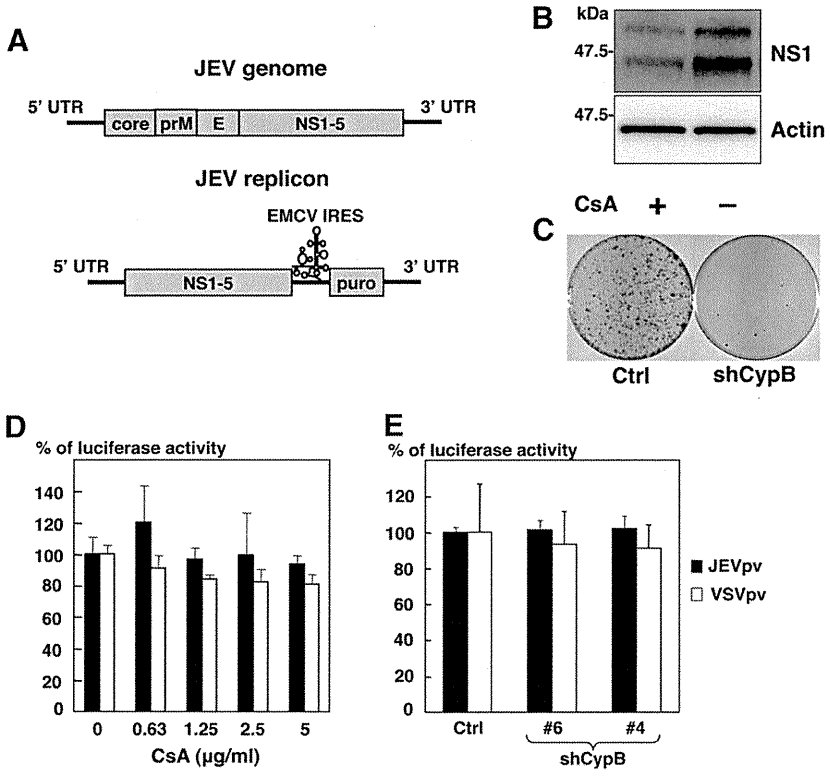

Fig. 5. CypB participates in the replication but not in the entry of JEV. (A) Schematic representations of the JEV genome and its subgenomic replicon. (B) JEV replicon cells were treated with CsA (1 μg/ml) for 6 days, and the expressions of NS1 and actin were detected by immunoblotting. (C) The stable CypB-knockdown and control cell lines were electroporated with the JEV replicon RNA and cultured for 3 weeks in the presence of 1 μg/ml of puromycin. The remaining cells were fixed with 4% paraformaldehyde and stained with crystal violet. (D) Huh7 cells treated with the indicated concentrations of CsA for 1 h were infected with the pseudotype viruses, JEVpv and VSVpv, and luciferase activities were determined at 24 h post-infection. (E) The stable CypB-knockdown and control cell lines were incubated with the pseudotype viruses, and the luciferase activities were determined. The results shown are representative of three independent assays, with error bars indicating standard deviations.

Cells and viruses

All cell lines were cultured at 37 °C under the condition of a humidified atmosphere and 5% CO_2. The human embryonic kidney cell line, 293T, African green monkey kidney cell line, Vero, hepatocellular carcinoma cell line, Huh7, mouse neural cell line, N18, and baby hamster kidney cell line, BHK, were maintained in Dulbecco's modified Eagle's medium (DMEM) (Sigma, St. Louis, MO) supplemented with 100 U/ml penicillin, 100 μg/ml streptomycin, non-essential amino acid (Sigma), and 10% fetal bovine serum (FBS). The mosquito C6/36 cell line (*Aedes albopictus*) was cultured at 27 °C and maintained in modified Eagle's medium (MEM) (Sigma). Huh7 cells were transfected with pSilencer-CypB or control plasmid and drug-resistant clones were selected by treatment with hygromycin B (Wako, Tokyo, Japan) at a final concentration of 50 μg/ml. Huh7 cells were electroporated with *in vitro*-transcribed RNA from pJErepIRESpuro and drug-resistant clones were selected by treatment with puromycin (InvivoGen, San Diego, CA) at a final concentration of 1 μg/ml. Wild-type JEV strain AT31 was used as described previously (Tani et al., 2010). The wild-type JEV was amplified on C6/36 cells and stored at −80 °C. Pseudotype VSVs bearing JEV PrM and E proteins (JEVpv) and VSVG (VSVpv) were produced in 293T cells transfected with pCAG105E and pCAGVSVG, respectively, as described previously (Tani et al., 2010). The infectivities of JEV and the pseudotype VSVs were assessed by both a focus-forming assay and luciferase activity as described previously (Tani et al., 2010). Cell viability was determined by using CellTiter-Glo (Promega Corporation, Madison, WI) according to the manufacturer's protocol.

Reagents and antibodies

CsA and FK506 were purchased from Sigma, and CsD and CsH from Eton Bioscience Inc. (San Diego, CA). Mouse monoclonal antibodies to tags of HA and FLAG and β-actin were previously described (Taguwa et al., 2009). Rabbit polyclonal antibodies to CypA and CypB were purchased from Upstate Cell Signaling (Lake Placid, NY) and Affinity BioReagents (Golden, CO), respectively. Rabbit polyclonal antibody to calnexin was purchased from Santa Cruz Biotechnology (Santa Cruz, CA). Mouse monoclonal antibody to JEV NS1 protein (34A1) was kindly provided by Dr. Yasui.

Transfection, immunoblotting, and immunoprecipitation

Transfection and immunoprecipitation were carried out as described previously (Taguwa et al., 2009). Immunoprecipitates boiled in loading buffer were subjected to 12.5% sodium dodecyl sulfate-polyacrylamide gel electrophoresis. The proteins were transferred to polyvinylidene

Fig. 6. NS4A protein recruits CypB to the replication complex in the JEV-infected cells. (A) FLAG-tagged CypB was co-expressed with HA-tagged NS1, NS2A, NS2B, NS3, NS4A, NS4B, or NS5 in 293T cells and immunoprecipitated with anti-HA antibody. The immunoprecipitates were subjected to immunoblotting by using either anti-FLAG or anti-HA antibody. (B) FLAG-tagged CypB was co-expressed with HA-tagged NS4A in 293T cells. The cell lysates obtained after lysis with the buffer containing CsA were immunoprecipitated with anti-FLAG antibody. The immunoprecipitates were subjected to immunoblotting by using either anti-FLAG or anti-HA antibody. (C) Huh7 cells transfected with an expression plasmid encoding HA-tagged NS4A or empty vector were fixed at 48 h post-transfection, permeabilized, and stained with the appropriate antibodies to HA (green), calnexin (red), and CypB (red). Cell nuclei were stained with DAPI (blue). Intracellular localization of CypB and NS4A was examined by confocal microscopy.

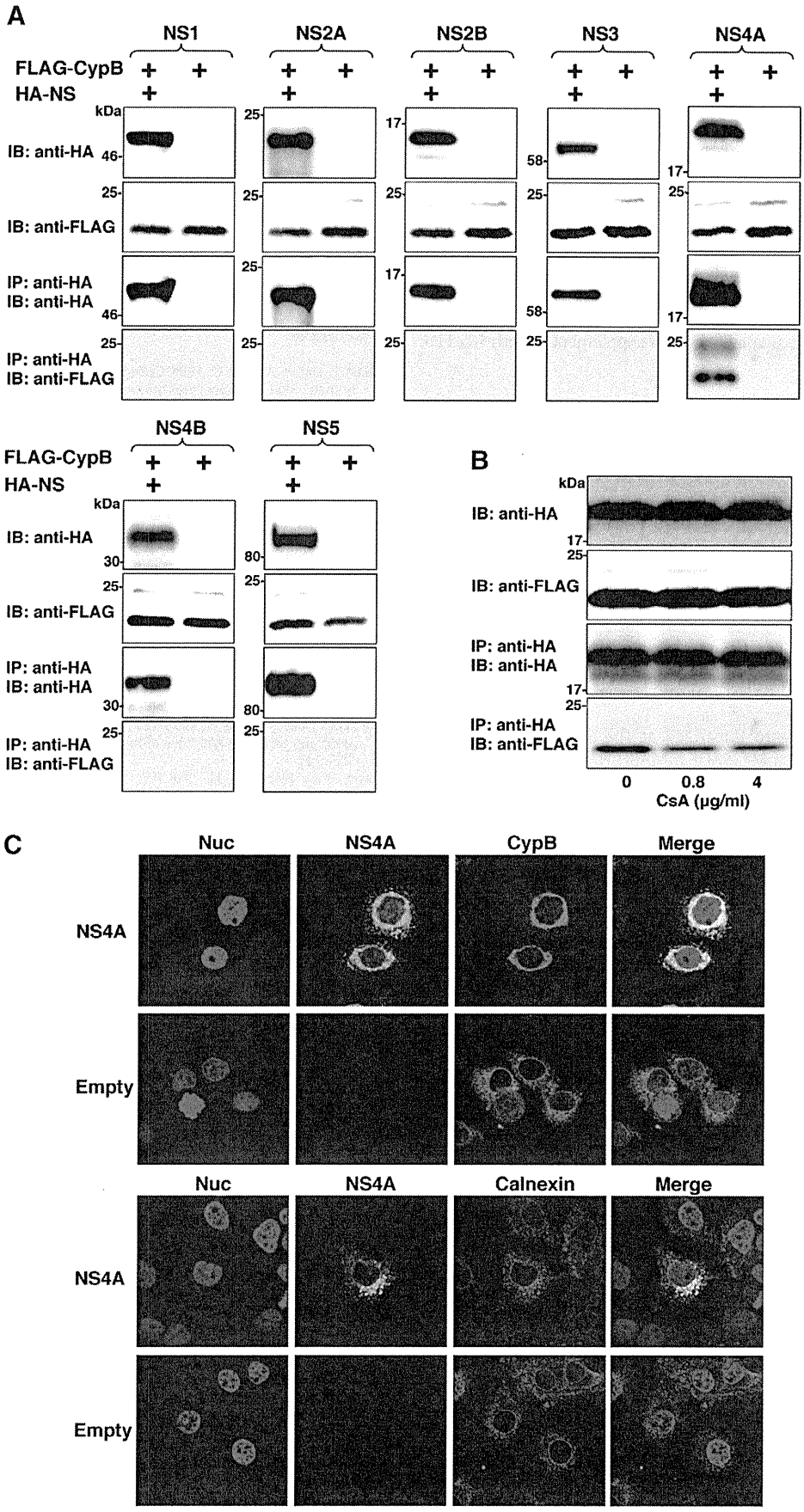
A
NS1
NS2A
NS2B
NS3
NS4A
FLAG-CypB
HA-NS
kDa
IB: anti-HA
IB: anti-FLAG
IP: anti-HA
IB: anti-HA
IP: anti-HA
IB: anti-FLAG
NS4B
NS5
B
CsA (μg/ml)
0
0.8
4
C
Nuc
NS4A
CypB
Merge
Empty
Calnexin

difluoride membranes (Millipore, Bedford, MA) and were reacted with the appropriate antibodies. The immune complexes were visualized with Super Signal West Femto substrate (Pierce, Rockford, IL) and detected by an LAS-3000 image analyzer system (Fujifilm, Tokyo, Japan).

Gene silencing by siRNA

The siRNAs against CypA and CypB were 5′-AAGCATACGGGTCCTGGCATC-3′ and 5′-AAGGTGGAGAGCACCAAGACA-3′, respectively (QIAGEN, Tokyo, Japan). FlexTube siRNAs against CypC and the negative control were purchased from QIAGEN. The cells were grown on 6-well plates and transfected with 35 nM siRNA by using Dharmafect (Dharmacon, Buckinghamshire, UK) according to the manufacturer's protocol. The transfected cells were incubated in DMEM supplemented with 10% FBS.

Quantitative RT-PCR

RNA was determined by the method described previously (Taguwa et al., 2009). The total RNA was prepared from cells by using an RNeasy mini kit (QIAGEN). First-strand cDNA was synthesized using an RNA LA PCR™ *in vitro* cloning kit (Takara Bio Inc.) and random primers. Each cDNA was determined by Platinum SYBR Green qPCR SuperMix UDG (Invitrogen, San Diego, CA) according to the manufacturer's protocol. Fluorescent signals were analyzed by an ABI PRISM 7000 (Applied Biosystems, Tokyo, Japan).

In vitro transcription and RNA transfection

Plasmid pJErepIRESpuro linearized at the *Swa* I site was transcribed *in vitro* using an mMESSAGE mMACHINE (Ambion) according to the manufacturer's protocol. The *in vitro*-transcribed RNA was introduced into Huh7 cells at 5 million cells/0.5 ml by electroporation at 270 V and 960 μF using Gene Pulser™ (Bio-rad, Hercules, CA).

Colony formation assay

Colony formation was determined as previously described (Taguwa et al., 2009). Briefly, *in vitro*-transcribed RNA was electroporated into Huh7 cells and plated on DMEM containing 10% FBS and non-essential amino acids. The medium was replaced with fresh DMEM containing 10% FBS, non-essential amino acids, and 1 μg/ml puromycin at 24 h post-transfection. The remaining colonies were fixed with 4% paraformaldehyde (PFA) and stained with crystal violet at 3 weeks after electroporation.

Indirect immunofluorescence assay

Cells cultured on glass slides were fixed with 4% PFA in phosphate buffered saline (PBS) at room temperature for 30 min. After washing three times with PBS, the cells were permeabilized for 20 min at room temperature with PBS containing 0.25% saponin and blocked with phosphate buffer containing 2% BSA for 1 h at room temperature. The cells were incubated with blocking buffer containing mouse anti-HA or rabbit anti-CypB at room temperature for 1 h, then washed three times with PBS and incubated with blocking buffer containing AF488-conjugated anti-mouse IgG and AF594-conjugated anti-rabbit IgG at room temperature for 1 h. Cell nuclei were stained blue with DAPI. Finally, the cells were washed three times with PBS and observed a FluoView FV1000 laser scanning confocal microscope (Olympus, Tokyo, Japan).

Statistical analysis

Results are expressed as the means ± standard deviation. The significance of differences between the means was determined by Student's *t*-test.

Acknowledgments

We thank H. Murase and M. Tomiyama for their secretarial work. This research was supported in part by grants-in-aid from the Ministry of Health, Labor, and Welfare; the Ministry of Education, Culture, Sports, Science, and Technology; and the Global Center of Excellence Program.

References

Allain, F., Denys, A., Spik, G., 1996. Cyclophilin B mediates cyclosporin A incorporation in human blood T-lymphocytes through the specific binding of complexed drug to the cell surface. Biochem. J. 317 (Pt 2), 565–570.
Almawi, W.Y., Melemedjian, O.K., 2000. Clinical and mechanistic differences between FK506 (tacrolimus) and cyclosporin A. Nephrol. Dial. Transplant. 15 (12), 1916–1918.
Andreotti, A.H., 2003. Native state proline isomerization: an intrinsic molecular switch. Biochemistry 42 (32), 9515–9524.
Bose, S., Mathur, M., Bates, P., Joshi, N., Banerjee, A.K., 2003. Requirement for cyclophilin A for the replication of vesicular stomatitis virus New Jersey serotype. J. Gen. Virol. 84 (Pt 7), 1687–1699.
Carpentier, M., Allain, F., Haendler, B., Denys, A., Mariller, C., Benaissa, M., Spik, G., 1999. Two distinct regions of cyclophilin B are involved in the recognition of a functional receptor and of glycosaminoglycans on T lymphocytes. J. Biol. Chem. 274 (16), 10990–10998.
Castro, A.P., Carvalho, T.M., Moussatche, N., Damaso, C.R., 2003. Redistribution of cyclophilin A to viral factories during vaccinia virus infection and its incorporation into mature particles. J. Virol. 77 (16), 9052–9068.
Chatterji, U., Bobardt, M., Selvarajah, S., Yang, F., Tang, H., Sakamoto, N., Vuagniaux, G., Parkinson, T., Gallay, P., 2009. The isomerase active site of cyclophilin A is critical for hepatitis C virus replication. J. Biol. Chem. 284 (25), 16998–17005.
Damaso, C.R., Moussatche, N., 1998. Inhibition of vaccinia virus replication by cyclosporin A analogues correlates with their affinity for cellular cyclophilins. J. Gen. Virol. 79 (Pt 2), 339–346.
Davis, W.G., Blackwell, J.L., Shi, P.Y., Brinton, M.A., 2007. Interaction between the cellular protein eEF1A and the 3′-terminal stem–loop of West Nile virus genomic RNA facilitates viral minus-strand RNA synthesis. J. Virol. 81 (18), 10172–10187.
Emara, M.M., Brinton, M.A., 2007. Interaction of TIA-1/TIAR with West Nile and dengue virus products in infected cells interferes with stress granule formation and processing body assembly. Proc. Natl Acad. Sci. USA 104 (21), 9041–9046.
Fernandes, F., Ansari, I.U., Striker, R., 2010. Cyclosporine inhibits a direct interaction between cyclophilins and hepatitis C NS5A. PLoS ONE 5 (3), e9815.
Franke, E.K., Yuan, H.E., Luban, J., 1994. Specific incorporation of cyclophilin A into HIV-1 virions. Nature 372 (6504), 359–362.
Gaither, L.A., Borawski, J., Anderson, L.J., Balabanis, K.A., Devay, P., Joberty, G., Rau, C., Schirle, M., Bouwmeester, T., Mickanin, C., Zhao, S., Vickers, C., Lee, L., Deng, G., Baryza, J., Fujimoto, R.A., Lin, K., Compton, T., Wiedmann, B., 2010. Multiple cyclophilins involved in different cellular pathways mediate HCV replication. Virology 397 (1), 43–55.
Galigniana, M.D., Morishima, Y., Gallay, P.A., Pratt, W.B., 2004. Cyclophilin-A is bound through its peptidylprolyl isomerase domain to the cytoplasmic dynein motor protein complex. J. Biol. Chem. 279 (53), 55754–55759.
Ghosh, D., Basu, A., 2009. Japanese encephalitis—a pathological and clinical perspective. PLoS Negl. Trop. Dis. 3 (9), e437.
Ho, S.N., Hunt, H.D., Horton, R.M., Pullen, J.K., Pease, L.R., 1989. Site-directed mutagenesis by overlap extension using the polymerase chain reaction. Gene 77 (1), 51–59.
Karlas, A., Machuy, N., Shin, Y., Pleissner, K.P., Artarini, A., Heuer, D., Becker, D., Khalil, H., Ogilvie, L.A., Hess, S., Maurer, A.P., Muller, E., Wolff, T., Rudel, T., Meyer, T.F., 2010. Genome-wide RNAi screen identifies human host factors crucial for influenza virus replication. Nature 463 (7282), 818–822.
Kaul, A., Stauffer, S., Berger, C., Pertel, T., Schmitt, J., Kallis, S., Zayas, M., Lohmann, V., Luban, J., Bartenschlager, R., 2009. Essential role of cyclophilin A for hepatitis C virus replication and virus production and possible link to polyprotein cleavage kinetics. PLoS Pathog. 5 (8), e1000546.
Kim, J., Choi, T.G., Ding, Y., Kim, Y., Ha, K.S., Lee, K.H., Kang, I., Ha, J., Kaufman, R.J., Lee, J., Choe, W., Kim, S.S., 2008. Overexpressed cyclophilin B suppresses apoptosis associated with ROS and Ca2+ homeostasis after ER stress. J. Cell Sci. 121 (Pt 21), 3636–3648.
Konig, R., Zhou, Y., Elleder, D., Diamond, T.L., Bonamy, G.M., Irelan, J.T., Chiang, C.Y., Tu, B.P., De Jesus, P.D., Lilley, C.E., Seidel, S., Opaluch, A.M., Caldwell, J.S., Weitzman, M. D., Kuhen, K.L., Bandyopadhyay, S., Ideker, T., Orth, A.P., Miraglia, L.J., Bushman, F.D., Young, J.A., Chanda, S.K., 2008. Global analysis of host–pathogen interactions that regulate early-stage HIV-1 replication. Cell 135 (1), 49–60.
Konig, R., Stertz, S., Zhou, Y., Inoue, A., Hoffmann, H.H., Bhattacharyya, S., Alamares, J.G., Tscherne, D.M., Ortigoza, M.B., Liang, Y., Gao, Q., Andrews, S.E., Bandyopadhyay, S., De

Jesus, P., Tu, B.P., Pache, L., Shih, C., Orth, A., Bonamy, G., Miraglia, L., Ideker, T., Garcia-Sastre, A., Young, J.A., Palese, P., Shaw, M.L., Chanda, S.K., 2010. Human host factors required for influenza virus replication. Nature 463 (7282), 813–817.
Limjindaporn, T., Wongwiwat, W., Noisakran, S., Srisawat, C., Netsawang, J., Puttikhunt, C., Kasinrerk, W., Avirutnan, P., Thiemmeca, S., Sriburi, R., Sittisombut, N., Malasit, P., Yenchitsomanus, P.T., 2009. Interaction of dengue virus envelope protein with endoplasmic reticulum-resident chaperones facilitates dengue virus production. Biochem. Biophys. Res. Commun. 379 (2), 196–200.
Lindenbach, B.D., Rice, C.M., 1999. Genetic interaction of flavivirus nonstructural proteins NS1 and NS4A as a determinant of replicase function. J. Virol. 73 (6), 4611–4621.
Liu, X., Sun, L., Yu, M., Wang, Z., Xu, C., Xue, Q., Zhang, K., Ye, X., Kitamura, Y., Liu, W., 2009. Cyclophilin A interacts with influenza A virus M1 protein and impairs the early stage of the viral replication. Cell. Microbiol. 11 (5), 730–741.
Mackenzie, J.M., Jones, M.K., Young, P.R., 1996. Immunolocalization of the dengue virus nonstructural glycoprotein NS1 suggests a role in viral RNA replication. Virology 220 (1), 232–240.
Mackenzie, J.M., Khromykh, A.A., Jones, M.K., Westaway, E.G., 1998. Subcellular localization and some biochemical properties of the flavivirus Kunjin nonstructural proteins NS2A and NS4A. Virology 245 (2), 203–215.
Mackenzie, J.M., Jones, M.K., Westaway, E.G., 1999. Markers for trans-Golgi membranes and the intermediate compartment localize to induced membranes with distinct replication functions in flavivirus-infected cells. J. Virol. 73 (11), 9555–9567.
Mackenzie, J.S., Gubler, D.J., Petersen, L.R., 2004. Emerging flaviviruses: the spread and resurgence of Japanese encephalitis, West Nile and dengue viruses. Nat. Med. 10 (12 Suppl), S98–S109.
Mackenzie, J.M., Khromykh, A.A., Parton, R.G., 2007. Cholesterol manipulation by West Nile virus perturbs the cellular immune response. Cell Host Microbe 2 (4), 229–239.
Miller, S., Krijnse-Locker, J., 2008. Modification of intracellular membrane structures for virus replication. Nat. Rev. Microbiol. 6 (5), 363–374.
Miller, S., Kastner, S., Krijnse-Locker, J., Buhler, S., Bartenschlager, R., 2007. The non-structural protein 4A of dengue virus is an integral membrane protein inducing membrane alterations in a 2K-regulated manner. J. Biol. Chem. 282 (12), 8873–8882.
Mori, Y., Yamashita, T., Tanaka, Y., Tsuda, Y., Abe, T., Moriishi, K., Matsuura, Y., 2007. Processing of capsid protein by cathepsin L plays a crucial role in replication of Japanese encephalitis virus in neural and macrophage cells. J. Virol. 81 (16), 8477–8487.
Nakagawa, M., Sakamoto, N., Tanabe, Y., Koyama, T., Itsui, Y., Takeda, Y., Chen, C.H., Kakinuma, S., Oooka, S., Maekawa, S., Enomoto, N., Watanabe, M., 2005. Suppression of hepatitis C virus replication by cyclosporin a is mediated by blockade of cyclophilins. Gastroenterology 129 (3), 1031–1041.
Price, E.R., Zydowsky, L.D., Jin, M.J., Baker, C.H., McKeon, F.D., Walsh, C.T., 1991. Human cyclophilin B: a second cyclophilin gene encodes a peptidyl-prolyl isomerase with a signal sequence. Proc. Natl Acad. Sci. USA 88 (5), 1903–1907.
Price, E.R., Jin, M., Lim, D., Pati, S., Walsh, C.T., McKeon, F.D., 1994. Cyclophilin B trafficking through the secretory pathway is altered by binding of cyclosporin A. Proc. Natl Acad. Sci. USA 91 (9), 3931–3935.
Puyang, X., Poulin, D.L., Mathy, J.E., Anderson, L.J., Ma, S., Fang, Z., Zhu, S., Lin, K., Fujimoto, R., Compton, T., Wiedmann, B., 2010. Mechanism of resistance of hepatitis C virus replicons to structurally distinct cyclophilin inhibitors. Antimicrob. Agents Chemother. 54 (5), 1981–1987.
Qing, M., Yang, F., Zhang, B., Zou, G., Robida, J.M., Yuan, Z., Tang, H., Shi, P.Y., 2009. Cyclosporine inhibits flavivirus replication through blocking the interaction between host cyclophilins and viral NS5 protein. Antimicrob. Agents Chemother. 53 (8), 3226–3235.
Reyes-Del Valle, J., Chavez-Salinas, S., Medina, F., Del Angel, R.M., 2005. Heat shock protein 90 and heat shock protein 70 are components of dengue virus receptor complex in human cells. J. Virol. 79 (8), 4557–4567.
Roosendaal, J., Westaway, E.G., Khromykh, A., Mackenzie, J.M., 2006. Regulated cleavages at the West Nile virus NS4A-2K-NS4B junctions play a major role in rearranging cytoplasmic membranes and Golgi trafficking of the NS4A protein. J. Virol. 80 (9), 4623–4632.
Rycyzyn, M.A., Clevenger, C.V., 2002. The intranuclear prolactin/cyclophilin B complex as a transcriptional inducer. Proc. Natl Acad. Sci. USA 99 (10), 6790–6795.
Sadeg, N., Pham-Huy, C., Rucay, P., Righenzi, S., Halle-Pannenko, O., Claude, J.R., Bismuth, H., Duc, H.T., 1993. In vitro and in vivo comparative studies on immunosuppressive properties of cyclosporines A, C, D and metabolites M1, M17 and M21. Immunopharmacol. Immunotoxicol. 15 (2–3), 163–177.
Silverman, J.A., Hayes, M.L., Luft, B.J., Joiner, K.A., 1997. Characterization of anti-Toxoplasma activity of SDZ 215-918, a cyclosporin derivative lacking immunosuppressive and peptidyl-prolyl-isomerase-inhibiting activity: possible role of a P glycoprotein in Toxoplasma physiology. Antimicrob. Agents Chemother. 41 (9), 1859–1866.
Solomon, T., Ni, H., Beasley, D.W., Ekkelenkamp, M., Cardosa, M.J., Barrett, A.D., 2003. Origin and evolution of Japanese encephalitis virus in southeast Asia. J. Virol. 77 (5), 3091–3098.
Sumiyoshi, H., Mori, C., Fuke, I., Morita, K., Kuhara, S., Kondou, J., Kikuchi, Y., Nagamatu, H., Igarashi, A., 1987. Complete nucleotide sequence of the Japanese encephalitis virus genome RNA. Virology 161 (2), 497–510.
Taguwa, S., Kambara, H., Omori, H., Tani, H., Abe, T., Mori, Y., Suzuki, T., Yoshimori, T., Moriishi, K., Matsuura, Y., 2009. Cochaperone activity of human butyrate-induced transcript 1 facilitates hepatitis C virus replication through an Hsp90-dependent pathway. J. Virol. 83 (20), 10427–10436.
Tai, A.W., Benita, Y., Peng, L.F., Kim, S.S., Sakamoto, N., Xavier, R.J., Chung, R.T., 2009. A functional genomic screen identifies cellular cofactors of hepatitis C virus replication. Cell Host Microbe 5 (3), 298–307.
Tani, H., Shiokawa, M., Kaname, Y., Kambara, H., Mori, Y., Abe, T., Moriishi, K., Matsuura, Y., 2010. Involvement of ceramide in the propagation of Japanese encephalitis virus. J. Virol. 84 (6), 2798–2807.
Thali, M., Bukovsky, A., Kondo, E., Rosenwirth, B., Walsh, C.T., Sodroski, J., Gottlinger, H. G., 1994. Functional association of cyclophilin A with HIV-1 virions. Nature 372 (6504), 363–365.
Wang, P., Heitman, J., 2005. The cyclophilins. Genome Biol. 6 (7), 226.
Watanabe, A., Yoneda, M., Ikeda, F., Terao-Muto, Y., Sato, H., Kai, C., 2010. CD147/EMMPRIN acts as a functional entry receptor for measles virus on epithelial cells. J. Virol. 84 (9), 4183–4193.
Watashi, K., Ishii, N., Hijikata, M., Inoue, D., Murata, T., Miyanari, Y., Shimotohno, K., 2005. Cyclophilin B is a functional regulator of hepatitis C virus RNA polymerase. Mol. Cell 19 (1), 111–122.
Wati, S., Soo, M.L., Zilm, P., Li, P., Paton, A.W., Burrell, C.J., Beard, M., Carr, J.M., 2009. Dengue virus infection induces upregulation of GRP78, which acts to chaperone viral antigen production. J. Virol. 83 (24), 12871–12880.
Welsch, S., Miller, S., Romero-Brey, I., Merz, A., Bleck, C.K., Walther, P., Fuller, S.D., Antony, C., Krijnse-Locker, J., Bartenschlager, R., 2009. Composition and three-dimensional architecture of the dengue virus replication and assembly sites. Cell Host Microbe 5 (4), 365–375.
Wu, S.F., Lee, C.J., Liao, C.L., Dwek, R.A., Zitzmann, N., Lin, Y.L., 2002. Antiviral effects of an iminosugar derivative on flavivirus infections. J. Virol. 76 (8), 3596–3604.
Yang, F., Robotham, J.M., Nelson, H.B., Irsigler, A., Kenworthy, R., Tang, H., 2008. Cyclophilin A is an essential cofactor for hepatitis C virus infection and the principal mediator of cyclosporine resistance in vitro. J. Virol. 82 (11), 5269–5278.
Zhang, J., Herscovitz, H., 2003. Nascent lipidated apolipoprotein B is transported to the Golgi as an incompletely folded intermediate as probed by its association with network of endoplasmic reticulum molecular chaperones, GRP94, ERp72, BiP, calreticulin, and cyclophilin B. J. Biol. Chem. 278 (9), 7459–7468.
Zhang, L., Mohan, P.M., Padmanabhan, R., 1992. Processing and localization of Dengue virus type 2 polyprotein precursor NS3-NS4A-NS4B-NS5. J. Virol. 66 (12), 7549–7554.

JOURNAL OF VIROLOGY, July 2011, p. 6882–6892 Vol. 85, No. 14
0022-538X/11/$12.00 doi:10.1128/JVI.02418-10

Hepatitis C Virus Hijacks P-Body and Stress Granule Components around Lipid Droplets[▽]

Yasuo Ariumi,[1,2]* Misao Kuroki,[1] Yukihiro Kushima,[3] Kanae Osugi,[4] Makoto Hijikata,[3] Masatoshi Maki,[4] Masanori Ikeda,[1] and Nobuyuki Kato[1]

Department of Tumor Virology, Okayama University Graduate School of Medicine, Dentistry, and Pharmaceutical Sciences, Okayama 700-8558, Japan[1]; Center for AIDS Research, Kumamoto University, Kumamoto 860-0811, Japan[2]; Department of Viral Oncology, Institute for Virus Research, Kyoto University, Kyoto 606-8507, Japan[3]; and Department of Applied Molecular Biosciences, Graduate School of Bioagricultural Sciences, Nagoya University, Nagoya 464-8601, Japan[4]

Received 19 November 2010/Accepted 21 April 2011

The microRNA miR-122 and DDX6/Rck/p54, a microRNA effector, have been implicated in hepatitis C virus (HCV) replication. In this study, we demonstrated for the first time that HCV-JFH1 infection disrupted processing (P)-body formation of the microRNA effectors DDX6, Lsm1, Xrn1, PATL1, and Ago2, but not the decapping enzyme DCP2, and dynamically redistributed these microRNA effectors to the HCV production factory around lipid droplets in HuH-7-derived RSc cells. Notably, HCV-JFH1 infection also redistributed the stress granule components GTPase-activating protein (SH3 domain)-binding protein 1 (G3BP1), ataxin-2 (ATX2), and poly(A)-binding protein 1 (PABP1) to the HCV production factory. In this regard, we found that the P-body formation of DDX6 began to be disrupted at 36 h postinfection. Consistently, G3BP1 transiently formed stress granules at 36 h postinfection. We then observed the ringlike formation of DDX6 or G3BP1 and colocalization with HCV core after 48 h postinfection, suggesting that the disruption of P-body formation and the hijacking of P-body and stress granule components occur at a late step of HCV infection. Furthermore, HCV infection could suppress stress granule formation in response to heat shock or treatment with arsenite. Importantly, we demonstrate that the accumulation of HCV RNA was significantly suppressed in DDX6, Lsm1, ATX2, and PABP1 knockdown cells after the inoculation of HCV-JFH1, suggesting that the P-body and the stress granule components are required for the HCV life cycle. Altogether, HCV seems to hijack the P-body and the stress granule components for HCV replication.

Hepatitis C virus (HCV) is the causative agent of chronic hepatitis, which progresses to liver cirrhosis and hepatocellular carcinoma. HCV is an enveloped virus with a positive single-stranded 9.6-kb RNA genome, which encodes a large polyprotein precursor of approximately 3,000 amino acid (aa) residues. This polyprotein is cleaved by a combination of the host and viral proteases into at least 10 proteins in the following order: core, envelope 1 (E1), E2, p7, nonstructural 2 (NS2), NS3, NS4A, NS4B, NS5A, and NS5B (12, 13, 21). The HCV core protein, a nucleocapsid, is targeted to lipid droplets (LDs), and the dimerization of the core protein by a disulfide bond is essential for the production of infectious virus (24). Recently, LDs have been found to be involved in an important cytoplasmic organelle for HCV production (26). Budding is an essential step in the life cycle of enveloped viruses. The endosomal sorting complex required for transport (ESCRT) system has been involved in such enveloped virus budding machineries, including that of HCV (5).

DEAD-box RNA helicases with ATP-dependent RNA-unwinding activities have been implicated in various RNA metabolic processes, including transcription, translation, RNA splicing, RNA transport, and RNA degradation (32). Previously, DDX3 was identified as an HCV core-interacting protein by yeast two-hybrid screening (25, 29, 43). Indeed, DDX3 is required for HCV RNA replication (3, 31). DDX6 (Rck/p54) is also required for HCV replication (16, 33). DDX6 interacts with an initiation factor, eukaryotic initiation factor 4E (eIF-4E), to repress the translational activity of mRNP (38). Furthermore, DDX6 regulates the activity of the decapping enzymes DCP1 and DCP2 and interacts directly with Argonaute-1 (Ago1) and Ago2 in the microRNA (miRNA)-induced silencing complex (miRISC) and is involved in RNA silencing. DDX6 localizes predominantly in the discrete cytoplasmic foci termed the processing (P) body. Thus, the P body seems to be an aggregate of translationally repressed mRNPs associated with the translation repression and mRNA decay machinery.

In addition to the P body, eukaryotic cells contain another type of RNA granule termed the stress granule (SG) (1, 6, 22, 30). SGs are aggregates of untranslating mRNAs in conjunction with a subset of translation initiation factors (eIF4E, eIF3, eIF4A, eIFG, and poly(A)-binding protein [PABP]), the 40S ribosomal subunits, and several RNA-binding proteins, including PABP, T cell intracellular antigen 1 (TIA-1), TIA-1-related protein (TIAR), and GTPase-activating protein (SH3 domain)-binding protein 1 (G3BP1). SGs regulate mRNA translation and decay as well as proteins involved in various aspects of mRNA metabolisms. SGs are cytoplasmic phase-dense structures that occur in eukaryotic cells exposed to various environmental stress, including heat, arsenite, viral infection, oxidative conditions, UV irradiation, and hypoxia. Impor-

* Corresponding author. Mailing address: Center for AIDS Research, Kumamoto University, 2-2-1 Honjo, Kumamoto 860-0811, Japan. Phone and fax: 81 96 373 6834. E-mail: ariumi@kumamoto-u.ac.jp.
▽ Published ahead of print on 4 May 2011.

tantly, several viruses target SGs and stress granule components for viral replication (10, 11, 34, 39). Recent studies suggest that SGs and the P body physically interact and that mRNAs may move between the two compartments (1, 6, 22, 28, 30).

miRNAs are a class of small noncoding RNA molecules ~21 to 22 nucleotides (nt) in length. miRNAs usually interact with 3′-untranslated regions (UTRs) of target mRNAs, leading to the downregulation of mRNA expression. Notably, the liver-specific and abundant miR-122 interacts with the 5′-UTR of the HCV RNA genome and facilitates HCV replication (15, 17, 19, 20, 31). Ago2 is at least required for the efficient miR-122 regulation of HCV RNA accumulation and translation (40). However, the molecular mechanism(s) for how DDX6 and miR-122 as well as DDX3 positively regulate HCV replication is not fully understood. Therefore, we investigated the potential role of P-body and stress granule components in HCV replication.

MATERIALS AND METHODS

Cell culture. 293FT cells were cultured in Dulbecco's modified Eagle's medium (DMEM; Invitrogen, Carlsbad, CA) supplemented with 10% fetal bovine serum (FBS). HuH-7-derived RSc cured cells, in which cell culture-generated HCV-JFH1 (JFH1 strain of genotype 2a) (37) could infect and effectively replicate, were cultured in DMEM with 10% FBS as described previously (3–5, 23).

Plasmid construction. To construct pcDNA3-FLAG-DDX6, a DNA fragment encoding DDX6 was amplified from total RNAs derived from RSc cells by reverse transcription (RT)-PCR using KOD-Plus DNA polymerase (Toyobo) and the following pairs of primers: 5′-CGGGATCCAAGATGAGCACGGCC AGAACAGAGAACCCTGTT-3′ (forward) and 5′-CCGCTCGAGTTAAGGT TTCTCATCTTCTACAGGCTCGCT-3′ (reverse). The obtained DNA fragments were subcloned into either BamHI-XhoI site of the pcDNA3-FLAG vector (2), and the nucleotide sequences were determined by BigDye termination cycle sequencing using an ABI Prism 310 genetic analyzer (Applied Biosystems, Foster City, CA).

RNA interference. The following small interfering RNAs (siRNAs) were used: human ATXN2/ATX2/ataxin-2 (siGENOME SMRT pool M-011772-01-005), human PABP1/PABPC1 (siGENOME SMRT pool M-019598-01-005), human Lsm1 (siGENOME SMRT pool M-005124-01-005), human Xrn1 (siGENOME SMRT pool M-013754-01-005), human G3BP1 (ON-TARGETplus SMRT pool L-012099-00-005), human PATL1 (siGENOME SMRT pool M-015591-00-005), and siGENOME nontargeting siRNA pool 1 (D-001206-13-05) (Dharmacon, Thermo Fisher Scientific, Waltham, MA), as a control. siRNAs (25 nM final concentration) were transiently transfected into RSc cells (3–5, 23) using Oligofectamine (Invitrogen) according to the manufacturer's instructions. Oligonucleotides with the following sense and antisense sequences were used for the cloning of short hairpin RNA (shRNA)-encoding sequences targeted to DDX6 (DDX6i) as well as the control nontargeting shRNA (shCon) in a lentiviral vector: 5′-GATCC CCGGAGGAACTAACTCTGAAGTTCAAGAGACTTCAGAGTTAGTTCCT CCTTTTTGGAAA-3′ (sense) and 5′-AGCTTTTCCAAAAAGGAGGAACTAA CTCTGAAGTCTCTTGAACTTCAGAGTTAGTTCCTCCGGG-3′ (antisense) for DDX6i and 5′-GATCCCCGAATCCAGAGGTAATCTACTTCAAGAGA GTAGATTACCTCTGGATTCTTTTTGGAAA-3′ (sense) and 5′-AGCTTTTC CAAAAAGAATCCAGAGGTAATCTACTCTCTTGAAGTAGATTACCTC TGGATTCGGG-3′ (antisense) for shCon. The oligonucleotides described above were annealed and subcloned into the BglII-HindIII site, downstream from an RNA polymerase III promoter of pSUPER (8), to generate pSUPER-DDX6i and pSUPER-shCon, respectively. To construct pLV-DDX6i and pLV-shCon, the BamHI-SalI fragments of the corresponding pSUPER plasmids were subcloned into the BamHI-SalI site of pRDI292, an HIV-1-derived self-inactivating lentiviral vector containing a puromycin resistance marker allowing for the selection of transduced cells (7). pLV-DDX3i, described previously (3), was used.

Lentiviral vector production. The vesicular stomatitis virus G protein (VSV-G)-pseudotyped HIV-1-based vector system was described previously (27, 44). The lentiviral vector particles were produced by the transient transfection of the second-generation packaging construct pCMV-ΔR8.91 (27, 44), the VSV-G-envelope-expressing plasmid pMDG2, as well as pRDI292 into 293FT cells with FuGene6 reagent (Roche Diagnostics, Mannheim, Germany).

HCV infection experiments. The supernatants were collected from cell culture-generated HCV-JFH1 (37)-infected RSc cells (3–5, 23) at 5 days postinfection and stored at −80°C after filtering through a 0.45-μm filter (Kurabo, Osaka, Japan) until use. For infection experiments with HCV-JFH1, RSc cells (1×10^5 cells/well) were plated onto 6-well plates and cultured for 24 h. We then infected the cells at a multiplicity of infection (MOI) of 1 or 4. The culture supernatants were collected at 24 h postinfection, and the levels of the core protein were determined by an enzyme-linked immunosorbent assay (ELISA) (Mitsubishi Kagaku Bio-Clinical Laboratories, Tokyo, Japan). Total RNA was also isolated from the infected cellular lysates by using an RNeasy minikit (Qiagen, Hilden, Germany) for analysis of intracellular HCV RNA. The infectivity of HCV-JFH1 in the culture supernatants was determined by a focus-forming assay at 48 h postinfection. HCV-JFH1-infected cells were detected by using anti-HCV core (CP-9 and CP-11 mixture).

Quantitative RT-PCR analysis. The quantitative RT-PCR analysis of HCV RNA was performed by real-time LightCycler PCR (Roche) as described previously (3–5, 14, 23). We used the following forward and reverse primer sets for the real-time LightCycler PCR: 5′-ATGAGTCATGTGGCAGTGGA-3′ (forward) and 5′-GCTGGCTGTACTTCCTCCAC-3′ (reverse) for DDX3, 5′-ATG AGCACGGCCAGAACAGA-3′ (forward) and 5′-TTGCTGTGTCTGTGTGC CCC-3′ (reverse) for DDX6, 5′-TGACGGGGTCACCCACACTG-3′ (forward) and 5′-AAGCTGTAGCCGCGCTCGGT-3′ (reverse) for β-actin, and 5′-AGA GCCATAGTGGTCTGCGG-3′ (forward) and 5′-CTTTCGCAACCCAACGC TAC-3′ (reverse) for HCV-JFH1.

Preparation of anti-PATL1 antibody. The anti-PATL1 antiserum was raised in rabbits using the glutathione *S*-transferase (GST)-fused PATL1 Ct (C-terminal region of PATL1, aa 450 to 770) as an antigen, and immunoglobulins were affinity purified by using the maltose-binding protein (MBP)-fused PATL1 Ct that was immobilized on an *N*-hydroxysuccinimide (NHS) column (GE Healthcare Bio-Sciences AB, Uppsala, Sweden).

Preparation of LDs. Lipid droplets (LDs) were prepared as described previously (26). Cells were pelleted by centrifugation at 1,500 rpm. The pellet was resuspended in hypotonic buffer (50 mM HEPES [pH 7.4], 1 mM EDTA, 2 mM $MgCl_2$) supplemented with a protease inhibitor cocktail (Nacalai Tesque, Kyoto, Japan) and was incubated for 10 min at 4°C. The suspension was homogenized with 30 strokes of a glass Dounce homogenizer using a tight-fitting pestle (Wheaton, Millville, NJ). A 1/10 volume of 10× isotonic buffer {0.2 M HEPES (pH 7.4), 1.2 M potassium acetate (KoAc), 40 mM magnesium acetate [$Mg(oAc)_2$], and 50 mM dithiothreitol (DTT)} was added to the homogenate. The nuclei were removed by centrifugation at 2,000 rpm for 10 min at 4°C. The supernatant was collected and centrifuged at 16,000 × *g* for 10 min at 4°C. The supernatant was mixed with an equal volume of 1.04 M sucrose in isotonic buffer (50 mM HEPES, 100 mM KCl, 2 mM $MgCl_2$, and protease inhibitor cocktail). The solution was set in a 13.2-ml Polyallomer centrifuge tube (Beckman Coulter, Brea, CA). One milliliter of isotonic buffer was loaded onto the sucrose mixture. The tube was centrifuged at 100,000 × *g* in an SW41Ti rotor (Beckman Coulter) for 1 h at 4°C. After the centrifugation, the LD fraction on the top of the gradient solution was recovered in phosphate-buffered saline (PBS). The collected LD fraction was used for Western blot analysis.

Western blot analysis. Cells were lysed in a buffer containing 50 mM Tris-HCl (pH 8.0), 150 mM NaCl, 4 mM EDTA, 1% Nonidet P-40, 0.1% sodium dodecyl sulfate (SDS), 1 mM DTT, and 1 mM phenylmethylsulfonyl fluoride. Supernatants from these lysates were subjected to SDS-polyacrylamide gel electrophoresis, followed by immunoblot analysis using anti-DDX3 (catalog no. 54257 [NT] and 5428 [IN]; Anaspec, San Jose, CA), anti-DDX6 (A300-460A; Bethyl Laboratories, Montgomery, TX), anti-adipose differentiation-related protein (ADFP; GTX110204; GeneTex, San Antonio, TX), anti-calnexin (NT; Stressgen, Ann Arbor, MI), anti-HCV core (CP-9 and CP-11; Institute of Immunology, Tokyo, Japan), anti-β-actin antibody (A5441; Sigma, St. Louis, MO), anti-ATX2/SCA2 antibody (A302-033A; Bethyl), anti-PABP (sc-32318 [10E10]; Santa Cruz Biotechnology, Santa Cruz, CA), anti-PABP (ab21060; Abcam, Cambridge, United Kingdom), anti-G3BP1 (611126; BD Transduction Laboratories, San Jose, CA), anti-LSM1 (LS-C97364, Life Span Biosciences, Seattle, WA), anti-HSP70 (610607; BD), anti-XRN1 (A300-443A; Bethyl), or anti-PATL1 antibody.

Immunofluorescence and confocal microscopic analysis. Cells were fixed in 3.6% formaldehyde in PBS, permeabilized in 0.1% NP-40 in PBS at room temperature, and incubated with anti-DDX3 antibody (54257 [NT] and 5428 [IN]; Anaspec), anti-DDX3X (LS-C64576; Life Span), anti-DDX6 (A300-460A; Bethyl), anti-HCV core (CP-9 and CP-11), anti-ATX2/SCA2 antibody (A302-033A; Bethyl), anti-ataxin-2 (611378; BD), anti-PABP (ab21060; Abcam), anti-G3BP1 (A302-033A; Bethyl), anti-LSM1 (LS-C97364; Life Span), anti-XRN1

(A300-443A; Bethyl), anti-Dcp2 (A302-597A; Bethyl), anti-human Ago2 (011-22033; Wako, Osaka, Japan), or anti-PATL1 antibody at a 1:300 dilution in PBS containing 3% bovine serum albumin (BSA) for 30 min at 37°C. The cells were then stained with fluorescein isothiocyanate (FITC)-conjugated anti-rabbit antibody (Jackson ImmunoResearch, West Grove, PA) at a 1:300 dilution in PBS containing BSA for 30 min at 37°C. Lipid droplets and nuclei were stained with borondipyrromethene (BODIPY) 493/503 (Molecular Probes, Invitrogen) and DAPI (4′,6-diamidino-2-phenylindole), respectively, for 15 min at room temperature. Following extensive washing in PBS, the cells were mounted onto slides using a mounting medium of 90% glycerin–10% PBS with 0.01% *p*-phenylenediamine added to reduce fading. Samples were viewed under a confocal laser scanning microscope (LSM510; Zeiss, Jena, Germany).

Statistical analysis. A statistical comparison of the infectivities of HCV in the culture supernatants between the knockdown cells and the control cells was performed by using the Student *t* test. *P* values of less than 0.05 were considered statistically significant. All error bars indicate standard deviations.

RESULTS

HCV infection hijacks the P-body components. To investigate the potential role of P-body components in the HCV life cycle, we first examined the alteration of the subcellular localization of DDX3 or DDX6 by HCV-JFH1 infection using confocal laser scanning microscopy as previously described (2), since both DDX3 and DDX6 were identified previously as P-body components (6). For this, we used HuH-7-derived RSc cells, in which cell culture-generated HCV-JFH1 (JFH1 strain of genotype 2a) (37) can infect and effectively replicate (3, 4, 23). HCV-JFH1-infected RSc cells at 60 h postinfection were stained with anti-HCV core antibody, anti-DDX3, and/or anti-DDX6. Lipid droplets (LDs) and nuclei were stained with BODIPY 493/503 and DAPI (4′,6-diamidino-2-phenylindole), respectively. Samples were viewed under a confocal laser scanning microscope. Although we observed that endogenous DDX3 localized in faint cytoplasmic foci in uninfected RSc cells, DDX3 relocalized, formed ringlike structures, and colocalized with the HCV core protein in response to HCV-JFH1 infection (Fig. 1A). On the other hand, endogenous DDX6 was localized in the evident cytoplasmic foci termed P bodies in the uninfected cells (Fig. 1A). DDX6 also relocalized, formed ringlike structures, and colocalized with the core protein in response to HCV-JFH1 infection (Fig. 1A). Although we failed to observe that most of the P bodies of DDX6 perfectly colocalized with DDX3 in uninfected RSc cells (Fig. 1B), we observed a few P bodies of DDX6 colocalized with DDX3 in the uninfected cells (Fig. 1B, arrowheads). Intriguingly, we found that endogenous DDX3 colocalized with endogenous DDX6 in HCV-JFH1-infected cells (Fig. 1B). To further confirm this finding, pHA-DDX3 (41) and pcDNA3-FLAG-DDX6 were cotransfected into 293FT cells. Consequently, we observed that hemagglutinin (HA)-DDX3 colocalized with FLAG-DDX6 in 293FT cells coexpressing HA-DDX3 and FLAG-DDX6 (Fig. 1B), suggesting cross talk of DDX3 with DDX6. Recently, LDs have been found to be involved in an important cytoplasmic organelle for HCV production (26). Indeed, both DDX3 and DDX6 were recruited around LDs in response to HCV infection, while these proteins did not colocalize with LDs in uninfected naïve RSc cells (Fig. 1C). Furthermore, both DDX3 and DDX6 accumulated in the LD fraction of the HCV-JFH1-infected RSc cells; however, we could not detect both proteins in the LD fraction from uninfected control cells (Fig. 1D), suggesting that DDX3 and DDX6 are recruited around LDs in response to HCV infection.

These results suggest that HCV-JFH1 infection disrupts P-body formation. Therefore, we further examined whether or not HCV-JFH1 disrupts the P-body formations of other microRNA effectors, including Ago2; the Sm-like protein Lsm1, which is a subunit of heptameric-ring Lsm1-7, involved in decapping; the 5′-to-3′ exonuclease Xrn1; the decapping activator PATL1; and the decapping enzyme DCP2 (6, 21, 30). As expected, HCV-JFH1 disrupted the P-body formations of Ago2, Lsm1, and Xrn1 as well as PATL1 (Fig. 2). Lsm1, Xrn1, or PATL1 relocalized, formed ringlike structures, and colocalized with the HCV core protein in response to HCV-JFH1 infection, whereas they were localized predominantly in P bodies in uninfected RSc cells (Fig. 2). In fact, we observed that DDX6 colocalized with Ago2, a P-body marker (Fig. 2). In contrast, HCV-JFH1 failed to disrupt the P-body formation of DCP2 (Fig. 2). Thus, these results suggest that HCV disrupts P-body formation through the hijacking of P-body components.

HCV hijacks stress granule components. Since Nonhoff et al. recently reported that DDX6 interacted with ataxin-2 (ATX2) (28), we examined the potential cross talk among DDX6, ATX2, and HCV. Although ATX2 and G3BP1, a well-known stress granule component (36), were dispersed in the cytoplasm at 37°C, both proteins formed discrete aggregates termed stress granules and colocalized with each other in response to heat shock at 43°C for 45 min, indicating that ATX2 is also stress granule component (Fig. 3A). We did not observe prominent colocalization between DDX6 and ATX2 at 37°C (Fig. 3B). In contrast, we found that DDX6 was recruited, juxtaposed, and partially colocalized with stress granules of ATX2 in response to heat shock at 43°C for 45 min in the uninfected RSc cells (Fig. 3B). Notably, ATX2 was recruited, formed the ring-like structures, and partially colocalized with DDX6 in response to HCV-JFH1 infection even at 37°C (Fig. 3B). Furthermore, we noticed that ATX2 was recruited around LDs in HCV-JFH1-infected cells at 72 h postinfection, while ATX2 did not colocalize with LDs in uninfected cells (Fig. 3C), suggesting the colocalization of ATX2 with the HCV core protein in infected cells. Indeed, ATX2 colocalized with the HCV core protein in HCV-JFH1-infected RSc cells at 37°C (Fig. 3D). Moreover, HCV-JFH1 infection induced the colocalization of the core protein with other stress granule components, G3BP1 or PABP1 as well as ATX2 (Fig. 4 and 5). To further confirm our findings, we examined the time course of the redistribution of DDX6 and G3BP1 after inoculation with HCV-JFH1. Consequently, we still detected the P-body formation of DDX6 and dispersed G3BP1 in the cytoplasm, and we did not observe a colocalization between the HCV core protein and DDX6 at 12 and 24 h postinfection (Fig. 4). In contrast, we found that the P-body formation of DDX6 began to be disrupted at 36 h postinfection (Fig. 4). Consistently, G3BP1 formed stress granules at 36 h postinfection (Fig. 4). We then noticed a ringlike formation of DDX6 or G3BP1 and colocalization with the HCV core protein after 48 h postinfection (Fig. 4), suggesting that the disruption of P-body formation and the hijacking of P-body and stress granule components occur in a late step of HCV infection.

We then examined whether or not HCV-JFH1 infection

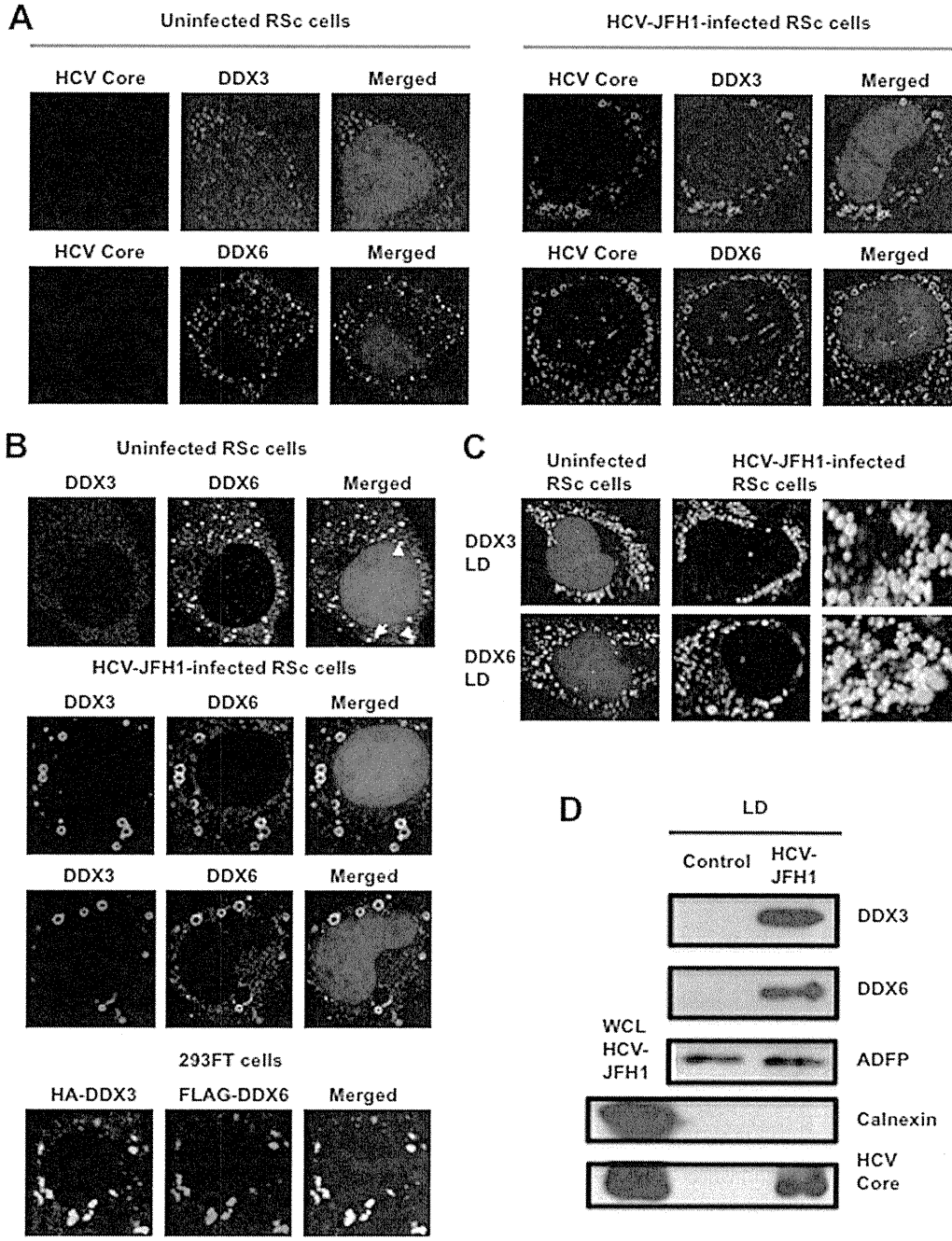

FIG. 1. Dynamic recruitment of DDX3 and DDX6 around lipid droplets (LDs) in response to HCV-JFH1 infection. (A) HCV-JFH1 disrupts the P-body formation of DDX6. Cells were fixed at 60 h postinfection and were then examined by confocal laser scanning microscopy. Cells were stained with anti-HCV core (CP-9 and CP-11 mixture) and either anti-DDX3 (54257 and 54258 mixture) or anti-DDX6 (A300-460A) antibody and then visualized with FITC (DDX3 or DDX6) or Cy3 (core). Images were visualized by using confocal laser scanning microscopy. The two-color overlay images are also exhibited (merged). Colocalization is shown in yellow. (B) HCV-JFH1 recruits DDX3 or DDX6 around LDs. Cells were stained with either anti-DDX3 or anti-DDX6 antibody and were then visualized with Cy3 (red). Lipid droplets and nuclei were stained with BODIPY 493/503 (green) and DAPI (blue), respectively. A high-magnification image is also shown. (C) Colocalization of DDX3 with DDX6. HCV-JFH1-infected RSc cells at 60 h postinfection were stained with anti-DDX3X (LS-C64576) and anti-DDX6 (A300-460A) antibodies. 293FT cells cotransfected with 100 ng of pcDNA3-FLAG-DDX6 and 100 ng of pHA-DDX3 (41) were stained with anti-FLAG-Cy3 and anti-HA-FITC antibodies (Sigma). (D) Association of DDX3 and DDX6 with LDs in response to HCV-JFH1 infection. The LD fraction and whole-cell lysates (WCL) were collected from uninfected RSc cells (control) or HCV-JFH1-infected RSc cells at 5 days postinfection. The results of Western blot analyses of DDX3, DDX6, and the HCV core protein as well as the LD marker ADFP and the endoplasmic reticulum (ER) marker calnexin in the LD fraction are shown.

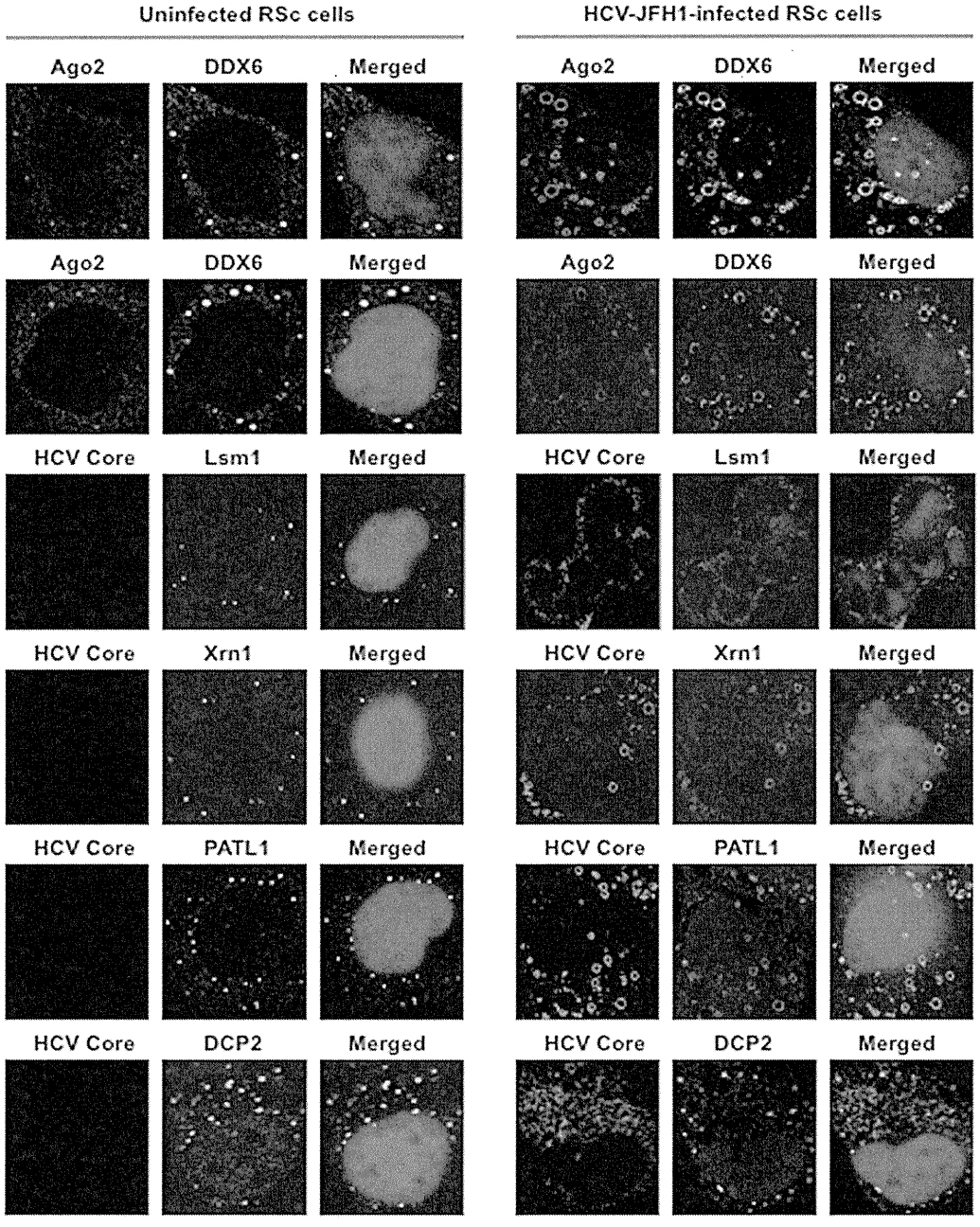

FIG. 2. HCV disrupts the P-body formation of microRNA effectors. Uninfected RSc cells and HCV-JFH1-infected RSc cells at 72 h postinfection were stained with anti-human AGO2 (011-22033) and anti-DDX6 (A300-460A) antibodies. The cells were also stained with anti-HCV core and anti-Lsm1 (LS-C97364), anti-Xrn1 (A300-443A), anti-PATL1, or anti-DCP2 (A302-597A) antibodies and were examined by confocal laser scanning microscopy.

could affect the stress granule formation of G3BP1, ATX2, or PABP1 in response to heat shock or treatment with arsenite. These stress granule components dispersed in the cytoplasm at 37°C, whereas these proteins formed stress granules in response to heat shock at 43°C for 45 min or treatment with 0.5 mM arsenite for 30 min (Fig. 5). In contrast, stress granules were not formed in HCV-JFH1-infected cells at 72 h postinfection in response to heat shock at 43°C for 45 min (Fig. 5), suggesting that HCV-JFH1 infection suppresses stress granule formation in response to heat shock or treatment with arsenite. Intriguingly, G3BP1, ATX2, or PABP1 still colocalized with the HCV core protein even under the above-described stress conditions (Fig. 5). Furthermore, Western blot analysis of cell lysates of uninfected or HCV-JFH1-infected cells at 72 h postinfection showed similar protein expression levels of ATX2, PABP1, HSP70, DDX3, DDX6, and Lsm1 but not G3BP1 (Fig. 6), suggesting that HCV-JFH1 infection does not affect host mRNA translation.

P-body and stress granule components are required for HCV replication. Finally, we investigated the potential role of

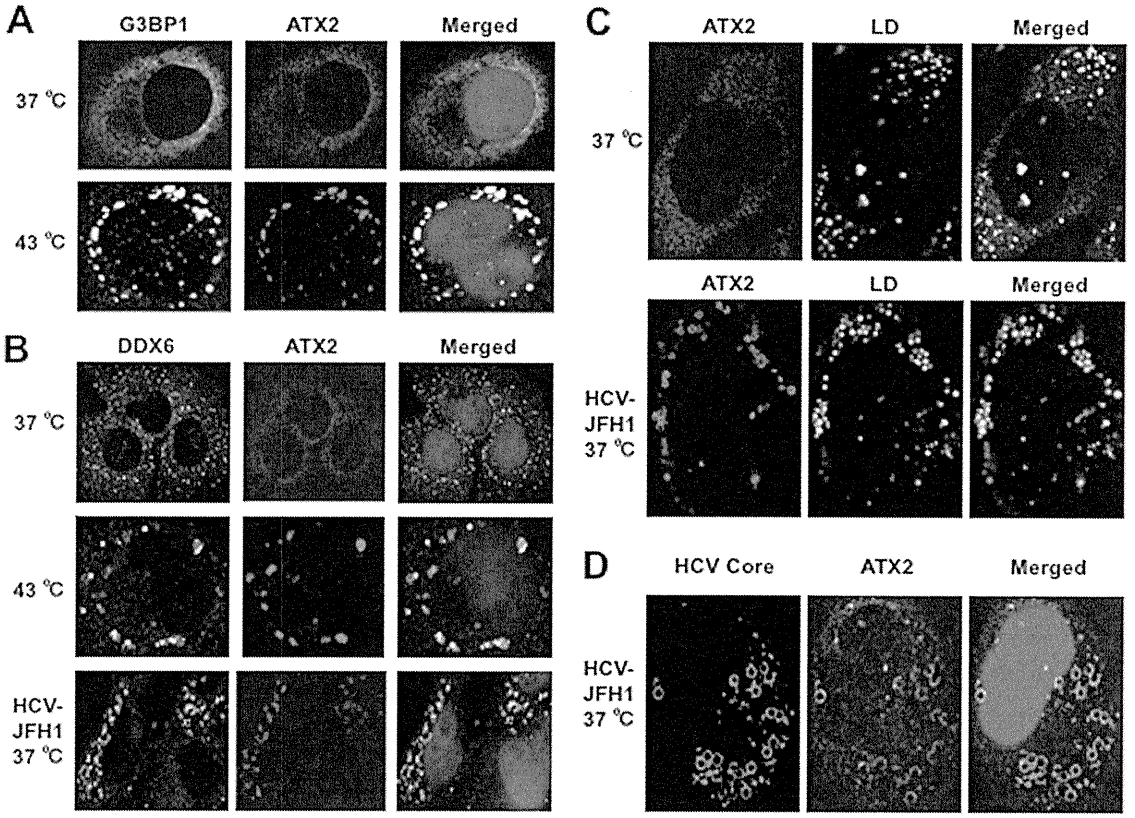

FIG. 3. Dynamic redistribution of ataxin-2 (ATX2) around LDs in response to HCV-JFH1 infection. (A) ATX2 is a stress granule component. RSc cells were incubated at 37°C or 43°C for 45 min. Cells were stained with anti-G3BP1 (A302-033A) and anti-ATX2 (A93520) antibodies and were examined by confocal laser scanning microscopy. (B) Dynamic redistribution of DDX6 and ATX2 in response to heat shock or HCV infection. RSc cells after heat shock at 43°C for 45 min or 72 h after inoculation with HCV-JFH1 were stained with anti-DDX6 and anti-ATX2 (A93520) antibodies. (C) HCV relocalizes ataxin-2 to LDs. HCV-JFH1-infected RSc cells at 72 h postinfection were stained with anti-ATX2 (A93520) antibody and BODIPY 493/503. (D) ATX2 colocalizes with the HCV core protein. HCV-JFH1-infected RSc cells at 72 h postinfection were stained with anti-ATX2/SCA2 (A301-118A) and anti-HCV core antibodies.

P-body and stress granule components in the HCV life cycle. We first used lentiviral vector-mediated RNA interference to stably knock down DDX6 as well as DDX3 in RSc cells. We used puromycin-resistant pooled cells 10 days after lentiviral transduction in all experiments. Real-time LightCycler RT-PCR analysis of DDX3 or DDX6 demonstrated a very effective knockdown of DDX3 or DDX6 in RSc cells transduced with lentiviral vectors expressing the corresponding shRNAs (Fig. 7A). Importantly, shRNAs did not affect cell viabilities (data not shown). We next examined the levels of HCV core and the infectivity of HCV in the culture supernatants as well as the level of intracellular HCV RNA in these knockdown cells 24 h after HCV-JFH1 infection at an MOI of 4. The results showed that the accumulation of HCV RNA was significantly suppressed in DDX3 or DDX6 knockdown cells (Fig. 7B). In this context, the release of the HCV core protein and the infectivity of HCV in the culture supernatants were also significantly suppressed in these knockdown cells (Fig. 7C and D). This finding suggested that DDX6 is required for HCV replication, like DDX3. To further examine the potential role of other P-body and stress granule components in HCV replication, we used RSc cells transiently transfected with a pool of siRNAs specific for ATX2, PABP1, Lsm1, Xrn1, G3BP1, and PATL1 as well as a pool of control siRNAs (siCon) following HCV-JFH1 infection. In spite of the very effective knockdown of each component (Fig. 7E), the siRNAs used in these experiments did not affect cell viabilities (data not shown). Consequently, the accumulation of HCV RNA was significantly suppressed in ATX2, PABP1, or Lsm1 knockdown cells (Fig. 7F), indicting that ATX2, PABP1, and Lsm1 are required for HCV replication. In contrast, the level of HCV RNA was not affected in Xrn1 knockdown cells (Fig. 7F), suggesting that Xrn1 is unrelated to HCV replication. Furthermore, we observed a moderate effect of siG3BP1 and siPATL1 on HCV RNA replication (Fig. 7F). Altogether, HCV seems to hijack the P-body and stress granule components around LDs for HCV replication.

DISCUSSION

So far, the P body and stress granules have been implicated in mRNA translation, RNA silencing, and RNA degradation as well as viral infection (1, 6, 22, 30). Host factors within the P body and stress granules can enhance or limit viral infection, and some viral RNAs and proteins accumulate in the P body and/or stress granules. Indeed, the microRNA effectors DDX6, GW182, Lsm1, and Xrn1 negatively regulate HIV-1 gene expression by preventing the association of viral mRNA

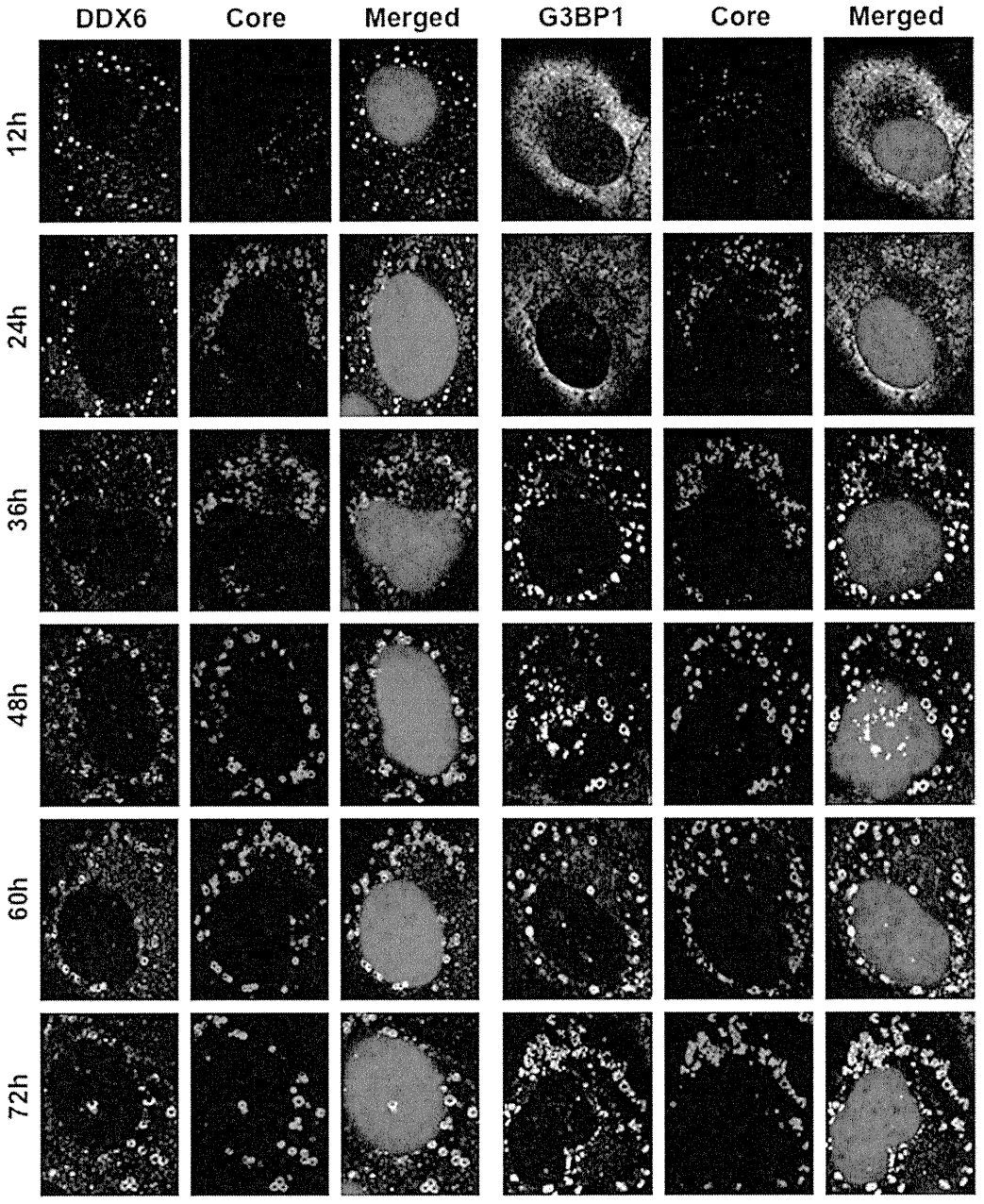

FIG. 4. Dynamic redistribution of DDX6 and G3BP1 in response to HCV-JFH1 infection. RSc cells at the indicated times (hours) after inoculation with HCV-JFH1 were stained with anti-HCV core and either anti-DDX6 (A300-460A) or anti-G3BP1 (A302-033A) antibodies.

with polysomes (9). In contrast, miRNA effectors such as DDX6, Lsm1, PatL1, and Ago2 positively regulate HCV replication (Fig. 7B and F) (16, 31, 33). We have also found that DDX3 and DDX6 are required for HCV RNA replication (3) (Fig. 7B) and that DDX3 colocalized with DDX6 in HCV-JFH1-infected RSc cells (Fig. 1B), suggesting that DDX3 comodulates the DDX6 function in HCV RNA replication. In this regard, the liver-specific miR-122 interacts with the 5′-UTR of the HCV RNA genome and positively regulates HCV replication (15, 17, 19, 20, 31). Since miRNAs usually interact with DDX6 and Ago2 in miRISC and are involved in RNA silencing, DDX6 and Ago2 may be required for miR-122-dependent HCV replication. Indeed, quite recently, a study showed that Ago2 is required for miR-122-dependent HCV RNA replication and translation (40). However, little is known regarding how miR-122 and DDX6 positively regulate HCV replication. Accordingly, we have shown that these miRNA effectors, including DDX6, Lsm1, Xrn1, and Ago2, accumulated around LDs and the HCV production factory and colocalized with the HCV core protein in response to HCV infection (Fig. 1 and 2). However, the decapping enzyme DCP2 did not accumulate and colocalize with the core protein (Fig. 2). Consistent with this finding, Scheller et al. reported previously that the depletion of DCP2 by siRNA did not affect HCV

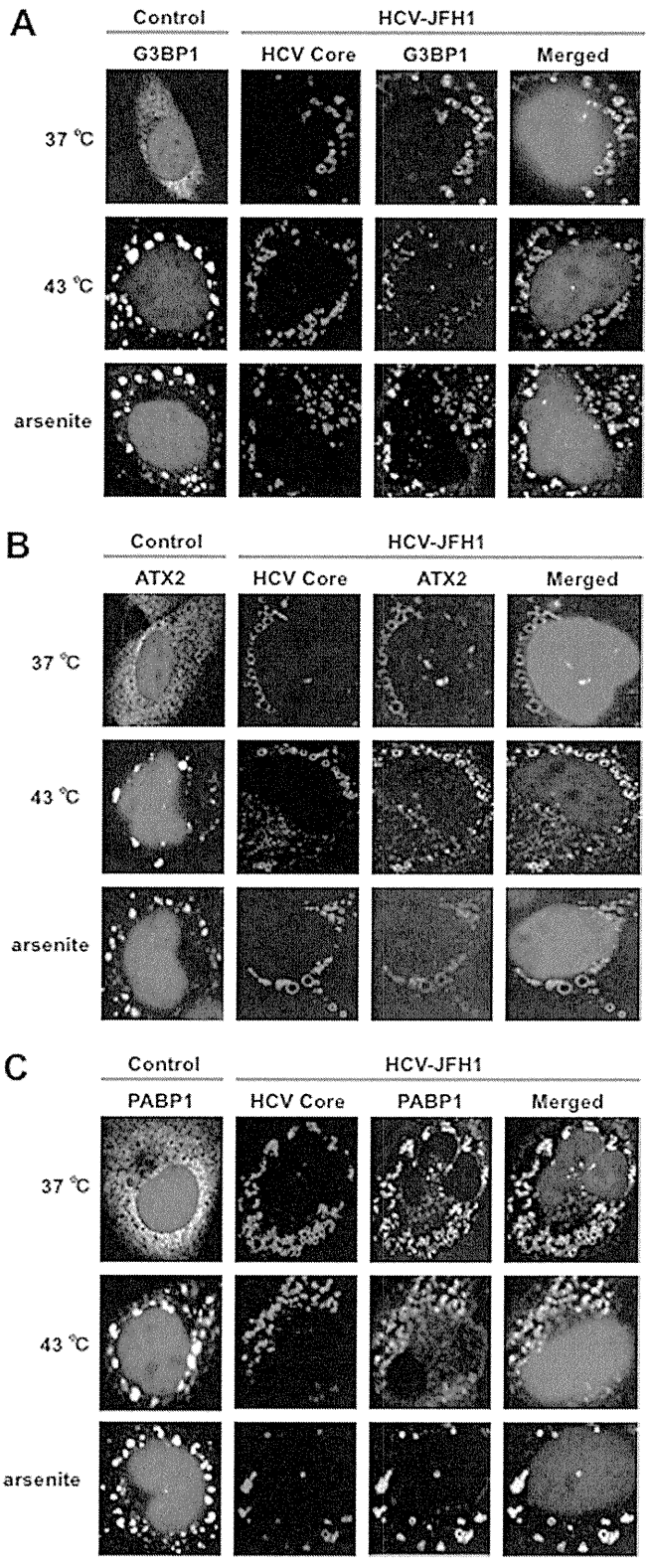

FIG. 5. HCV suppresses stress granule formation in response to heat shock or treatment with arsenite. Naïve RSc cells or HCV-JFH1-infected RSc cells at 72 h postinfection were incubated at 37°C or 43°C for 45 min. Cells were also treated with 0.5 mM arsenite for 30 min. Cells were stained with anti-HCV core and anti-G3BP1 (A), anti-ATX2 (B), or anti-PABP1 (ab21060) (C) antibodies and were examined by confocal laser scanning microscopy.

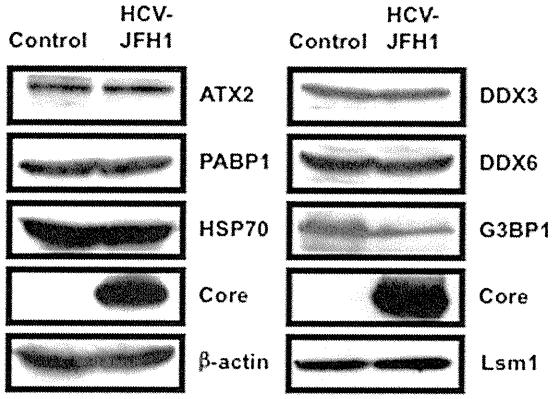

FIG. 6. Host protein expression levels in response to HCV-JFH1 infection. The results of the Western blot analyses of cellular lysates with anti-ATX2/SCA2 antibody (A301-118A), anti-PABP1 (ab21060), anti-HSP70 (610607), anti-HCV core, anti-β-actin, anti-DDX3 (54257 [NT] and 5428 [IN] mixture), anti-DDX6 (A300-460A), anti-G3BP1 (611126), or anti-LSM1 (LS-C97364) antibody in HCV-JFH1-infected RSc cells at 72 h postinfection as well as in naïve RSc cells are shown.

production (33). Since HCV harbors the internal ribosome entry site (IRES) structure in the 5′-UTR of the HCV genome instead of a cap structure, unlike HIV-1, DCP2 may not be recruited on the HCV genome and utilized for HCV replication. Otherwise, DCP2 may determine whether or not DDX6 and miRNAs positively or negatively regulate target mRNA.

Furthermore, we have demonstrated that HCV infection hijacks the P-body and stress granule components around LDs (Fig. 1, 2, 4, and 5). We have found that the P-body formation of DDX6 began to be disrupted at 36 h postinfection (Fig. 4). Consistently, G3BP1 formed stress granules at 36 h postinfection. We then observed the ringlike formation of DDX6 or G3BP1 and colocalization with the HCV core protein after 48 h postinfection, suggesting that the disruption of P-body formation and the hijacking of P-body and stress granule components occur at a late step of HCV infection. Furthermore, HCV infection could suppress stress granule formation in response to heat shock or treatment with arsenite (Fig. 5). In this regard, West Nile virus and dengue virus, of the family *Flaviviridae*, interfere with stress granule formation and P-body assembly through interactions with T cell intracellular antigen 1 (TIA-1)/TIAR (11). Moreover, PABP1 and G3BP1, stress granule components, are known to be common viral targets for the inhibition of host mRNA translation (34, 39). In fact, HIV-1 and poliovirus proteases cleave PABP1 and/or G3BP1 and suppress stress granule formation during viral infection (34, 39). On the other hand, HCV infection transiently induced stress granules at 36 h postinfection (Fig. 4) and did not cleave PABP1 (Fig. 6); however, HCV could suppress stress granule formation in response to heat shock or treatment with arsenite through hijacking their components around LDs, the HCV production factory (Fig. 5). Consistently, Jones et al. showed that HCV transiently induces stress granules of enhanced green fluorescent protein (EGFP)-G3BP at 36 h after infection with the cell culture-generated HCV (HCVcc) reporter virus Jc1FLAG2 (p7-nsGluc2A); however, those authors did not show the recruitment of EGFP-G3BP to LDs (18). Although we do not know the exact reason for this apparent discrepancy,

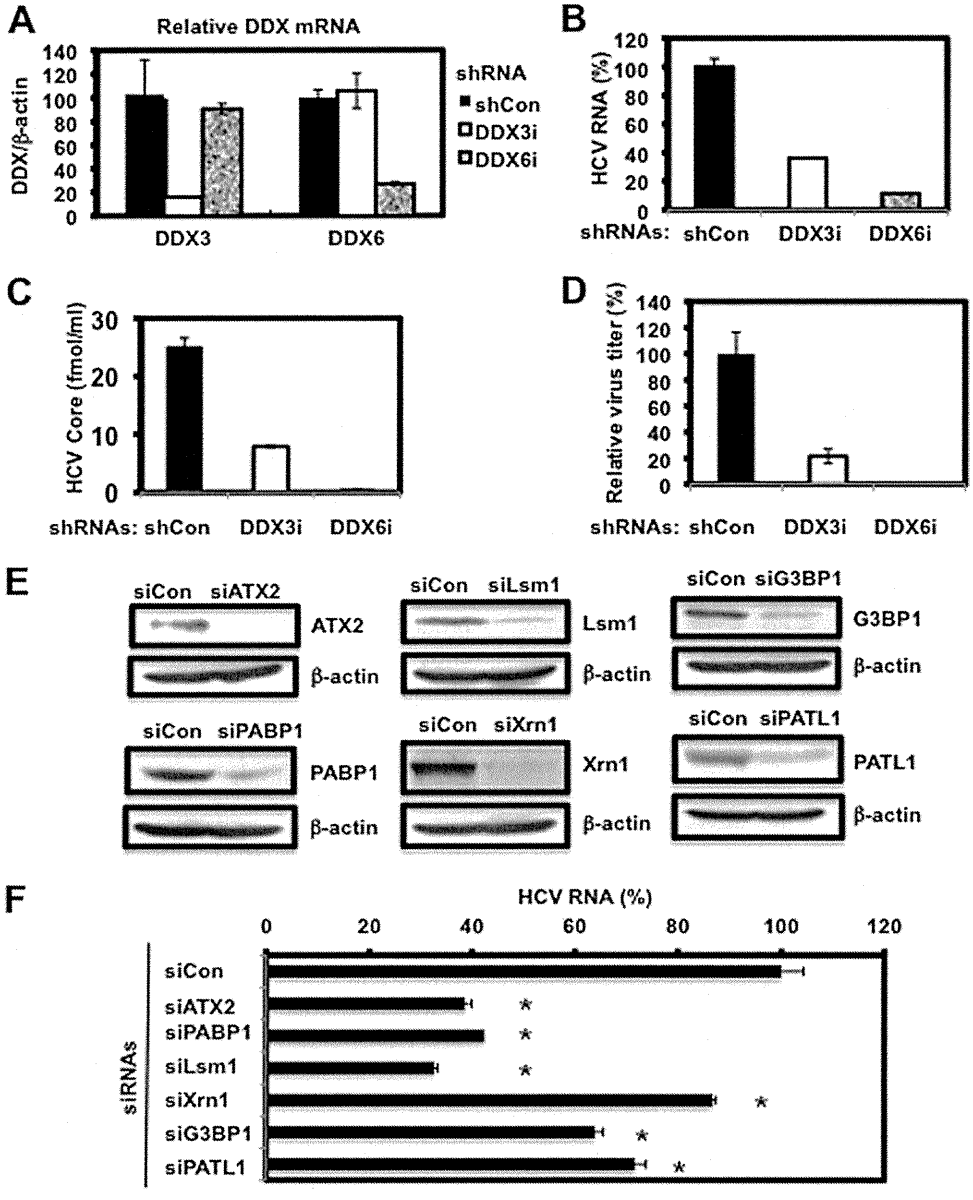

FIG. 7. Requirement of P-body and stress granule components for HCV replication. (A) Inhibition of DDX3 or DDX6 mRNA expression by the shRNA-producing lentiviral vector. Real-time LightCycler RT-PCR for DDX3 or DDX6 was also performed for β-actin mRNA in RSc cells expressing shRNA targeted to DDX3 (DDX3i) or DDX6 (DDX6i) or the control nontargeting shRNA (shCon) in triplicate. Each mRNA level was calculated relative to the level in RSc cells transduced with the control nontargeting lentiviral vector (shCon), which was assigned as 100%. Error bars in this panel and other panels indicate standard deviations. (B) Levels of intracellular genome-length HCV-JFH1 RNA in the cells at 24 h postinfection at an MOI of 4 were monitored by real-time LightCycler RT-PCR. Results from three independent experiments are shown. Each HCV RNA level was calculated relative to the level in RSc cells transduced with a control lentiviral vector (shCon), which was assigned as 100%. (C) The levels of HCV core in the culture supernatants from the stable knockdown RSc cells 24 h after inoculation of HCV-JFH1 at an MOI of 4 were determined by ELISA. Experiments were done in triplicate, and columns represent the mean core protein levels. (D) The infectivity of HCV in the culture supernatants from stable-knockdown RSc cells 24 h after inoculation of HCV-JFH1 at an MOI of 4 was determined by a focus-forming assay at 24 h postinfection. Experiments were done in triplicate, and each virus titer was calculated relative to the level in RSc cells transduced with a control lentiviral vector (shCon), which was assigned as 100%. (E) Inhibition of ATX2, PABP1, Lsm1, Xrn1, G3BP1, or PATL1 protein expression by 72 h after transient transfection of RSc cells with a pool of control nontargeting siRNA (siCon) or a pool of siRNAs specific for ATX2, PABP1, Lsm1, Xrn1, G3BP1, or PATL1 (25 nM), respectively. The results of Western blot analyses of cellular lysates with anti-ATX2, anti-PABP1, anti-Lsm1, anti-Xrn1, anti-G3BP1, anti-PATL1, or anti-β-actin antibody are shown. (F) Levels of intracellular genome-length HCV-JFH1 RNA in the cells at 48 h postinfection at an MOI of 1 were monitored by real-time LightCycler RT-PCR. RSc cells were transiently transfected with a pool of control siRNA (siCon) or a pool of siRNAs specific for ATX2, PABP1, Lsm1, Xrn1, G3BP1, and PATL1 (25 nM). At 48 h after transfection, the cells were inoculated with HCV-JFH1 at an MOI of 1 and incubated for 2 h. The culture medium was then changed and incubated for 22 h. Experiments were done in triplicate, and each HCV RNA level was calculated relative to the level in RSc cells transfected with a control siRNA (siCon), which was assigned as 100%. Asterisks indicate significant differences compared to the control treatment (*, $P < 0.01$).

several possible explanations can be offered. First, those authors examined the localization of EGFP-G3BP within 48 h postinfection, and we observed it at later times (Fig. 4). Second, they used only EGFP-tagged G3BP instead of endogenous G3BP1. Third, they used a Jc1FLAG2 (p7-nsGluc2A) clone, and an HCV-JFH1 clone could markedly induce the recruitment of the core protein to LDs compared to that of Jc1. Also, Jangra et al. failed to observe the recruitment of DDX6 to LDs at 2 days after infection with HJ3-5 virus (16). Accordingly, we also observed that most of the DDX6 still formed intact P bodies at earlier times (12 h or 24 h postinfection). Importantly, we observed the recruitment of DDX6 to LDs 48 h later (Fig. 4). Furthermore, those authors did not show the ringlike structure formation of the HJ3-5 core protein around LDs, unlike the JFH1 core protein that we used in this study. The interaction of the HCV core protein with DDX6 may explain the recruitment of P-body components to LDs. However, we do not yet know whether the P-body function(s) can be performed on LDs. At least, HCV infection did not affect the translation of several host mRNAs with 5′ caps and 3′ poly(A) tails despite the disruption of P-body formation at 72 h postinfection (Fig. 6), suggesting that HCV does not affect P-body function and that HCV recruits functional P bodies to LDs.

We need to address the potential role of stress granule components, such as PABP1, in HCV replication/translation, since the HCV genome does not harbor the 3′ poly(A) tail. Intriguingly, we have found that the accumulation of HCV RNA was significantly suppressed in PABP1 knockdown RSc cells (Fig. 7F). In this regard, Tingting et al. demonstrated previously that G3BP1 and PABP1 as well as DDX1 were identified as the HCV 3′-UTR RNA-binding proteins by proteomic analysis and that G3BP1 was required for HCV RNA replication (35). Yi et al. also reported that G3BP1 was associated with HCV NS5B and that G3BP1 was required for HCV RNA replication (42). We observed a moderate effect of siG3BP1 on HCV RNA replication (Fig. 7F). In contrast, the accumulation of HCV RNA was significantly suppressed in ATX2 and Lsm1 knockdown cells as well as in PABP1 knockdown cells (Fig. 7F), suggesting that ATX2, Lsm1, and PABP1 are required for HCV replication.

Taking these results together, this study has demonstrated for the first time that HCV hijacks P-body and stress granule components around LDs. This hijacking may regulate HCV RNA replication and translation. Indeed, we have found that the accumulation of genome-length HCV-O (genotype 1b) (14) RNA was markedly suppressed in DDX6 knockdown O cells (data not shown). More importantly, these P-body and stress granule components may be involved in the maintenance of the HCV RNA genome without 5′ cap and 3′ poly(A) tail structures in the cytoplasm for long periods, since the hijacking of P-body and stress granule components by HCV occurred at later times.

ACKNOWLEDGMENTS

We thank D. Trono for the lentiviral vector system, T. Wakita for HCV-JFH1, and K. T. Jeang for pHA-DDX3. We also thank T. Nakamura and K. Takeshita for their technical assistance.

This work was supported by a grant-in-aid for scientific research (C) from the Japan Society for the Promotion of Science (JSPS); by a grant-in-aid for research on hepatitis from the Ministry of Health, Labor, and Welfare of Japan; and by the Viral Hepatitis Research Foundation of Japan. M.K. was supported by a research fellowship from the JSPS for young scientists.

REFERENCES

1. **Anderson, P., and N. Kedersha.** 2007. Stress granules: the Tao of RNA triage. Trends Biochem. Sci. **33**:141–150.
2. **Ariumi, Y., et al.** 2003. Distinct nuclear body components, PML and SMRT, regulate the *trans*-acting function of HTLV-1 Tax oncoprotein. Oncogene **22**:1611–1619.
3. **Ariumi, Y., et al.** 2007. DDX3 DEAD-box RNA helicase is required for hepatitis C virus RNA replication. J. Virol. **81**:13922–13926.
4. **Ariumi, Y., et al.** 2008. The DNA damage sensors ataxia-telangiectasia mutated kinase and checkpoint kinase 2 are required for hepatitis C virus RNA replication. J. Virol. **82**:9639–9646.
5. **Ariumi, Y., et al.** 2011. The ESCRT system is required for hepatitis C virus production. PLoS One **6**:e14517.
6. **Beckham, C. J., and R. Parker.** 2008. P bodies, stress granules, and viral life cycles. Cell Host Microbe **3**:206–212.
7. **Bridge, A. J., S. Pebernard, A. Ducraux, A. L. Nicoulaz, and R. Iggo.** 2003. Induction of an interferon response by RNAi vectors in mammalian cells. Nat. Genet. **34**:263–264.
8. **Brummelkamp, T. R., R. Bernard, and R. Agami.** 2002. A system for stable expression of short interfering RNAs in mammalian cells. Science **296**:550–553.
9. **Chable-Bessia, C., et al.** 2009. Suppression of HIV-1 replication by microRNA effectors. Retrovirology **6**:26.
10. **Cristea, I. M., et al.** 2010. Host factors associated with the Sindbis virus RNA-dependent RNA polymerase: role for G3BP1 and G3BP2 in virus replication. J. Virol. **84**:6720–6732.
11. **Emara, M. M., and M. A. Brinton.** 2007. Interaction of TIA-1/TIAR with West Nile and dengue virus products in infected cells interferes with stress granule formation and processing body assembly. Proc. Natl. Acad. Sci. U. S. A. **104**:9041–9046.
12. **Hijikata, M., N. Kato, Y. Ootsuyama, M. Nakagawa, and K. Shimotohno.** 1991. Gene mapping of the putative structural region of the hepatitis C virus genome by in vitro processing analysis. Proc. Natl. Acad. Sci. U. S. A. **88**:5547–5551.
13. **Hijikata, M., et al.** 1993. Proteolytic processing and membrane association of putative nonstructural proteins of hepatitis C virus. Proc. Natl. Acad. Sci. U. S. A. **90**:10773–10777.
14. **Ikeda, M., et al.** 2005. Efficient replication of a full-length hepatitis C virus genome, strain O, in cell culture, and development of a luciferase reporter system. Biochem. Biophys. Res. Commun. **329**:1350–1359.
15. **Jangra, R. K., M. Yi, and S. M. Lemon.** 2010. Regulation of hepatitis C virus translation and infectious virus production by the microRNA miR-122. J. Virol. **84**:6615–6625.
16. **Jangra, R. K., M. Yi, and S. M. Lemon.** 2010. DDX6 (Rck/p54) is required for efficient hepatitis C virus replication but not IRES-directed translation. J. Virol. **84**:6810–6824.
17. **Ji, H., et al.** 2008. MicroRNA-122 stimulates translation of hepatitis C virus RNA. EMBO J. **27**:3300–3310.
18. **Jones, C. T., et al.** 2010. Real-time imaging of hepatitis C virus infection using a fluorescent cell-based reporter system. Nat. Biotechnol. **28**:167–171.
19. **Jopling, C. L., M. Yi, A. M. Lancaster, S. M. Lemon, and P. Sarnow.** 2005. Modulation of hepatitis C virus RNA abundance by a liver-specific microRNA. Science **309**:1577–1581.
20. **Jopling, C. L., S. Schütz, and P. Sarnow.** 2008. Position-dependent function for a tandem microRNA miR-122-binding site located in the hepatitis C virus RNA genome. Cell Host Microbe **4**:77–85.
21. **Kato, N., et al.** 1990. Molecular cloning of the human hepatitis C virus genome from Japanese patients with non-A, non-B hepatitis. Proc. Natl. Acad. Sci. U. S. A. **87**:9524–9528.
22. **Kedersha, N., and P. Anderson.** 2007. Mammalian stress granules and processing bodies. Methods Enzymol. **431**:61–81.
23. **Kuroki, M., et al.** 2009. Arsenic trioxide inhibits hepatitis C virus RNA replication through modulation of the glutathione redox system and oxidative stress. J. Virol. **83**:2338–2348.
24. **Kushima, Y., T. Wakita, and M. Hijikata.** 2010. A disulfide-bonded dimer of the core protein of hepatitis C virus is important for virus-like particle production. J. Virol. **84**:9118–9127.
25. **Mamiya, N., and H. J. Worman.** 1999. Hepatitis C virus core protein binds to a DEAD box RNA helicase. J. Biol. Chem. **274**:15751–15756.
26. **Miyanari, Y., et al.** 2007. The lipid droplet is an important organelle for hepatitis C virus production. Nat. Cell Biol. **9**:1089–1097.
27. **Naldini, L., et al.** 1996. In vivo gene delivery and stable transduction of nondividing cells by a lentiviral vector. Science **272**:263–267.
28. **Nonhoff, U., et al.** 2007. Ataxin-2 interacts with the DEAD/H-box RNA helicase DDX6 and interferes with P-bodies and stress granules. Mol. Biol. Cell **18**:1385–1396.
29. **Owsianka, A. M., and A. H. Patel.** 1999. Hepatitis C virus core protein interacts with a human DEAD box protein DDX3. Virology **257**:330–340.

30. **Parker, R., and U. Sheth.** 2007. P bodies and the control of mRNA translation and degradation. Mol. Cell **25:**635–646.
31. **Randall, G., et al.** 2007. Cellular cofactors affecting hepatitis C virus infection and replication. Proc. Natl. Acad. Sci. U. S. A. **104:**12884–12889.
32. **Rocak, S., and P. Linder.** 2004. DEAD-box proteins: the driving forces behind RNA metabolism. Nat. Rev. Mol. Cell Biol. **5:**232–241.
33. **Scheller, N., et al.** 2009. Translation and replication of hepatitis C virus genomic RNA depends on ancient cellular proteins that control mRNA fates. Proc. Natl. Acad. Sci. U. S. A. **106:**13517–13522.
34. **Smith, R. W., and N. K. Gray.** 2010. Poly(A)-binding protein (PABP): a common viral target. Biochem. J. **426:**1–11.
35. **Tingting, P., F. Caiyun, Y. Zhigang, Y. Pengyuan, and Y. Zhenghong.** 2006. Subproteomic analysis of the cellular proteins associated with the 3′ untranslated region of the hepatitis C virus genome in human liver cells. Biochem. Biophys. Res. Commun. **347:**683–691.
36. **Tourrière, H., et al.** 2003. The RasGAP-associated endoribonuclease G3BP assembles stress granules. J. Cell Biol. **160:**823–831.
37. **Wakita, T., et al.** 2005. Production of infectious hepatitis C virus in tissue culture from a cloned viral genome. Nat. Med. **11:**791–796.
38. **Weston, A., and J. Sommerville.** 2006. Xp54 and related (DDX6-like) RNA helicase: roles in messenger RNP assembly, translation regulation and RNA degradation. Nucleic Acids Res. **34:**3082–3094.
39. **White, J. P., A. M. Cardenas, W. E. Marissen, and R. E. Lloyd.** 2007. Inhibition of cytoplasmic mRNA stress granule formation by a viral proteinase. Cell Host Microbe **2:**295–305.
40. **Wilson, J. A., C. Zhang, A. Huys, and C. D. Richardson.** 2011. Human Ago2 is required for efficient miR-122 regulation of HCV RNA accumulation and translation. J. Virol. **85:**2342–2350.
41. **Yedavalli, V. S., C. Neuveut, Y. H. Chi, L. Kleiman, and K. T. Jeang.** 2004. Requirement of DDX3 DAED box RNA helicase for HIV-1 Rev-RRE export function. Cell **119:**381–392.
42. **Yi, Z., et al.** 2006. Subproteomic study of hepatitis C virus replicon reveals Ras-GTPase-activating protein binding protein 1 as potential HCV RC component. Biophys. Biochem. Res. Commun. **350:**174–178.
43. **You, L. R., et al.** 1999. Hepatitis C virus core protein interacts with cellular putative RNA helicase. J. Virol. **73:**2841–2853.
44. **Zufferey, R., D. Nagy, R. J. Mandel, L. Naldini, and D. Trono.** 1997. Multiply attenuated lentiviral vector achieves efficient gene delivery in vivo. Nat. Biotechnol. **15:**871–875.

Virus Research 157 (2011) 61–70

Contents lists available at ScienceDirect

Virus Research

journal homepage: www.elsevier.com/locate/virusres

Mechanism of action of ribavirin in a novel hepatitis C virus replication cell system

Kyoko Mori[a], Masanori Ikeda[a], Yasuo Ariumi[a], Hiromichi Dansako[a], Takaji Wakita[b], Nobuyuki Kato[a,*]

[a] Department of Tumor Virology, Okayama University Graduate School of Medicine, Dentistry, and Pharmaceutical Sciences, 2-5-1 Shikata-cho, Okayama 700-8558, Japan
[b] Department of Virology II, National Institute of Infectious Diseases, 1-23-1 Toyama, Shinjuku-ku, Tokyo 162-8640, Japan

ARTICLE INFO

Article history:
Received 16 November 2010
Received in revised form 4 February 2011
Accepted 4 February 2011
Available online 12 February 2011

Keywords:
HCV
HCV RNA replication system
RBV
IMPDH inhibitor

ABSTRACT

Ribavirin (RBV) is a potential partner of interferon (IFN)-based therapy for patients with chronic hepatitis C. However, to date, its anti-hepatitis C virus (HCV) mechanism remains ambiguous due to the marginal activity of RBV on HCV RNA replication in HuH-7-derived cells, which are currently used as the only cell culture system for robust HCV replication. We investigated the anti-HCV activity of RBV using novel cell assay systems. The recently discovered human hepatoma cell line, Li23, which enables robust HCV replication, and the recently developed Li23-derived drug assay systems (ORL8 and ORL11), in which the genome-length HCV RNA (O strain of genotype 1b) encoding renilla luciferase efficiently replicates, were used for this study. At clinically achievable concentrations, RBV unexpectedly inhibited HCV RNA replication in ORL8 and ORL11 systems, but not in OR6 (an HuH-7-derived assay system). The anti-HCV activity of RBV was almost cancelled by an inhibitor of equilibrative nucleoside transporters. The evaluation of the anti-HCV mechanisms of RBV proposed to date using ORL8 ruled out the possibility that RBV induces error catastrophe, the IFN-signaling pathway or oxidative stress. However, we found that the anti-HCV activity of RBV was efficiently cancelled with guanosine, and demonstrated that HCV RNA replication was notably suppressed in inosine monophosphate dehydrogenase (IMPDH)-knockdown cells, suggesting that the antiviral activity of RBV is mediated through the inhibition of IMPDH. In conclusion, we demonstrated for the first time that inhibition of IMPDH is a major antiviral target by which RBV at clinically achievable concentrations inhibits HCV RNA replication.

1. Introduction

Hepatitis C virus (HCV) infection causes chronic hepatitis, which often leads to liver cirrhosis and hepatocellular carcinoma (Thomas, 2000). Since approximately 170 million people are infected with HCV worldwide, HCV infection is a serious global health problem (Thomas, 2000). HCV is an enveloped positive single-stranded RNA virus of the *Flaviviridae* family. The HCV genome encodes a large polyprotein precursor of approximately 3000 amino acids, which is cleaved into in the following order: Core, envelope 1 (E1), E2, p7, non-structural protein 2 (NS2), NS3, NS4A, NS4B, NS5A, and NS5B (Kato et al., 1990).

The current standard therapy for patients with chronic hepatitis C is a combination of pegylated-interferon (PEG-IFN) and ribavirin (RBV). This treatment currently achieves a sustained virological response (SVR) greater than 50% (Chevaliez et al., 2007). However, the mechanism of RBV activity in patients with chronic hepatitis C is still ambiguous. To date, five distinct mechanisms have been proposed: (a) RBV acts as an RNA mutagen that causes mutations of the HCV RNA genome and induces a so-called "error catastrophe" (Feld and Hoofnagle, 2005); (b) RBV enhances the IFN-signaling pathway (Feld et al., 2010; Thomas et al., 2011); (c) RBV induces GTP depression by inhibiting inosine monophosphate dehydrogenase (IMPDH) (Zhou et al., 2003); (d) RBV directly inhibits NS5B-encoded RNA-dependent RNA polymerase (Feld and Hoofnagle, 2005); (e) RBV enhances host T-cell mediated immunity by switching the T-cell phenotype from type 2 to type 1 (Lau et al., 2002). Unfortunately, no groups have clarified the anti-HCV mechanism of RBV at clinically achievable concentrations (5–14 μM) (Feld et al., 2010; Pawlotsky et al., 2004; Tanabe et al.,

Abbreviations: HCV, hepatitis C virus; E1, envelope 1; NS2, nonstructural protein 2; PEG, polyethylene glycol; IFN, interferon; RBV, ribavirin; SVR, sustained virological response; IMPDH, inosine monophosphate dehydrogenase; RL, renilla luciferase; EC_{50}, 50% effective concentration; VE, vitamin E; NBMPR, *S*-(4-nitrobenzyl)-6-thioinosine; MPA, mycophenolic acid; CsA, cyclosporine A; STAT1, signal transducer and activator of transcription 1; ENT, equilibrative nucleoside transporter; RT-PCR, reverse-transcription polymerase chain reaction; ISG, IFN-stimulated gene; IRF7, IFN regulatory factor 7; IP-10, IFN-gamma-inducible protein-10; GAPDH, glyceraldehyde-3-phosphate dehydrogenase; 5′-UTR, 5′-untranslated region; Neo^R, neomycin-resistance gene; CNT, concentrative nucleoside transporter; EC_{90}, 90% effective concentration; CFE, colony-forming efficiency; MMPD, merimepodib.

* Corresponding author. Tel.: +81 86 235 7385; fax: +81 86 235 7392.
E-mail address: nkato@md.okayama-u.ac.jp (N. Kato).

0168-1702/$ – see front matter © 2011 Elsevier B.V. All rights reserved.
doi:10.1016/j.virusres.2011.02.005

2004). Although most of the above mechanisms were proposed based on studies using HuH-7 (human hepatoma cell line)-derived cells, which are currently used as the only cell culture system for robust HCV replication, the effective concentrations (50–1000 μM) of RBV were much higher than the clinically achievable concentrations (Feld and Hoofnagle, 2005; Feld et al., 2010; Lau et al., 2002; Pawlotsky et al., 2004; Thomas et al., 2011; Zhou et al., 2003). Indeed, our HuH-7-derived cell assay system (OR6) (Ikeda et al., 2005; Naka et al., 2005), in which genome-length HCV RNA (O strain of genotype 1b) encoding renilla luciferase (RL) efficiently replicates, also showed that the 50% effective concentration (EC_{50}) of RBV was approximately 100 μM (Naka et al., 2005).

Recently, we found a new human hepatoma cell line, Li23, that enables robust HCV RNA replication (Kato et al., 2009). We showed by microarray analysis that Li23 cells possessed expression profiles rather different from those in HuH-7 cells (Kato et al., 2009), and that the expression profile of Li23 cells was distinct from those of frequently used other hepatoma cell lines (Mori et al., 2010). We further developed Li23-derived cell culture assay systems (ORL8 and ORL11) in which genome-length HCV RNA (O strain of genotype 1b) encoding RL efficiently replicates (Kato et al., 2009). Here, we unexpectedly observed through the use of these cell culture assay systems the first evidence of anti-HCV activity of RBV at clinically achievable concentrations, and obtained the convincing data that the anti-HCV mechanism of RBV is mediated through the inhibition of IMPDH.

2. Materials and methods

2.1. Cell cultures

HuH-7-derived cells harboring an HCV replicon or genome-length HCV RNA were maintained with medium containing G418 (0.3 mg/ml) as described previously (Ikeda et al., 2005). Li23-derived polyclonal sORL8 and sORL11 cells harboring an HCV replicon were established by the transfection of ORN/3-5B/QR,KE,SR RNA (Kato et al., 2009) into the cured OL8 and OL11 cells, respectively. Li23-derived cells harboring an HCV replicon or genome-length HCV RNA were maintained as described previously (Kato et al., 2009). Cured cells, from which the HCV RNA had been eliminated by IFN treatment, were also maintained as described previously (Kato et al., 2009).

2.2. RL assay

RL assay was performed as described previously (Ikeda et al., 2005; Kato et al., 2009). The experiments were performed at least in triplicate.

2.3. Reagents

RBV was kindly provided by Yamasa (Chiba, Japan). Human IFN-α, vitamin E (VE), phloridzin dihydrate, *S*-(4-nitrobenzyl)-6-thioinosine (NBMPR), and mycophenolic acid (MPA) were purchased from Sigma–Aldrich (St. Louis, MO). Cyclosporine A (CsA) was purchased from Calbiochem (San Diego, CA). Guanosine and adenosine were purchased from Wako Pure Chemical Industries, Ltd. (Osaka, Japan).

2.4. Cell viability

Cell viability was examined by the method described previously (Kato et al., 2009). The experiments were performed in triplicate.

2.5. Western blot analysis

The preparation of cell lysates, sodium dodecyl sulfate–polyacrylamide gel electrophoresis and immunoblotting analysis with a PVDF membrane were performed as previously described (Kato et al., 2003). The antibodies used in this study were those against Core (CP11; Institute of Immunology, Tokyo, Japan), NS5B (a generous gift from Dr. M. Kohara, Tokyo Metropolitan Institute of Medical Science), signal transduction and activator of transcription 1 (STAT1) and phospho-STAT1 (Tyr701) (BD Transduction Laboratories, Lexington, KY) and equilibrative nucleoside transporter 1 (ENT1) (Abgent, San Diego, CA). β-actin antibody (Sigma–Aldrich) was used as the control for the amount of protein loaded per lane. Immunocomplexes were detected by using a Renaissance enhanced chemiluminescence assay (Perkin Elmer Life Sciences, Boston, MA).

2.6. Reverse transcription-polymerase chain reaction (RT-PCR)

Total RNA from the cultured cells was extracted with an RNeasy Mini Kit (Qiagen, Valencia, CA). RT-PCR was performed by a method described previously (Dansako et al., 2003) using the following primer pairs: IFN-stimulated gene (ISG) 15 (346 bp), 5′-GCCTTCCAGCAGCGTCTGGC-3′ and 5′-GCAGGCGCAGATTCATGAACACGG-3′; IFN regulatory factor 7 (IRF7) (221 bp), 5′-AGCTGCGCTACACGGAGGAACTG-3′ and 5′-CCACCAGCTCTTGGAAGAAGAC-3′; IFN-gamma-inducible protein-10 (IP-10) (111 bp), 5′-GGCCATCAAGAATTTACTGAAAGCA-3′ and 5′-TCTGTGTGGTCCATCCTTGGAA-3′; ENT1 (382 bp), 5′-GAGTTTCA-GTCTCCAACTCTCAG-3′ and 5′-GCATCGTGCTCGAAGACCACAG-3′; ENT2 (306 bp), 5′-CTTGTGTTGGTCTTCACAGTCAC-3′ and 5′-GGTGATGAAGTAGGCATCCTGTG-3′; ENT3 (350 bp), 5′-GTCTTCTTCATCACCAGCCTCATC-3′ and 5′-GTGCTGAGGTAGCCGT-TGCTGAG-3′; glyceraldehyde-3-phosphate dehydrogenase (GAPDH) (334 bp), 5′-GACTCATGACCACAGTCCATGC-3′ and 5′-GAGGAGACCACCTGGTGCTCAG-3′.

2.7. Infection of cells with secreted HCV

The inoculum was prepared from HCV-JFH1 (Wakita et al., 2005)-infected HuH-7-derived RSc cells (Ariumi et al., 2007; Kato et al., 2009) at 5 days postinfection and then stored at −80 °C after filtering through a 0.20-μm filter (Kurabo, Osaka, Japan) until use. ORL8c or RSc cells (each 5×10^4) were cultured for 24 h before infection. The cells were infected with 50 μl (equivalent to a multiplicity of infection of 0.05–0.1) of inoculum and maintained for several days until RBV treatment.

2.8. Quasispecies analysis of HCV RNA

ORL8 cells were treated with or without RBV (50 μM) for 72 h. Total RNA from the cultured cells was extracted with an RNeasy Mini Kit (Qiagen). To amplify genome-length HCV RNA, RT-PCR was performed separately in two fragments using KOD-plus DNA polymerase (Toyobo) as described previously (Ikeda et al., 2005; Kato et al., 2003). The two PCR products (the 6.0 kb region covering 5′-untranslated region (5′-UTR) to NS3 and the 6.1 kb region covering NS2 to NS5B) were subcloned into the *Xba*I site of pBR322MC, and sequence analysis of the region encoding RL to the neomycin-resistance gene (Neo^R) (1953 nts), NS5A (1341 nts), or NS5B (1773 nts) was performed as described previously (Ikeda et al., 2005). Synonymous and nonsynonymous substitutions at variance with the parental ORN/C-5B/QR,KE,SR sequences (Kato et al., 2009) were determined. To examine the error frequency of KOD-plus DNA polymerase in the PCR amplification, PCR using the plasmid containing ORN/C-5B/QR,KE,SR sequences was performed separately in the